Review

Voltage Stability of Power Systems with Renewable-Energy Inverter-Based Generators: A Review

Nasser Hosseinzadeh [1,*] **, Asma Aziz** [2] **, Apel Mahmud** [1] **, Ameen Gargoom** [1] **and Mahbub Rabbani** [1]

1   Centre for Smart Power and Energy Research, School of Engineering, Faculty of Science, Engineering, and Built Environment, Deakin University, Geelong, VIC 3216, Australia; apel.mahmud@deakin.edu.au (A.M.); a.gargoom@deakin.edu.au (A.G.); m.rabbani@deakin.edu.au (M.R.)
2   School of Engineering, Edith Cowan University, Perth, WA 6027, Australia; asma.aziz@ecu.edu.au
*   Correspondence: nasser.hosseinzadeh@deakin.edu.au; Tel.: +61-3522-73815

Abstract: The main purpose of developing microgrids (MGs) is to facilitate the integration of renewable energy sources (RESs) into the power grid. RESs are normally connected to the grid via power electronic inverters. As various types of RESs are increasingly being connected to the electrical power grid, power systems of the near future will have more inverter-based generators (IBGs) instead of synchronous machines. Since IBGs have significant differences in their characteristics compared to synchronous generators (SGs), particularly concerning their inertia and capability to provide reactive power, their impacts on the system dynamics are different compared to SGs. In particular, system stability analysis will require new approaches. As such, research is currently being conducted on the stability of power systems with the inclusion of IBGs. This review article is intended to be a preface to the Special Issue on Voltage Stability of Microgrids in Power Systems. It presents a comprehensive review of the literature on voltage stability of power systems with a relatively high percentage of IBGs in the generation mix of the system. As the research is developing rapidly in this field, it is understood that by the time that this article is published, and further in the future, there will be many more new developments in this area. Certainly, other articles in this special issue will highlight some other important aspects of the voltage stability of microgrids.

Keywords: voltage stability; electrical power system stability; microgrid; inverter based generator; inverter based resources; reactive power; renewable energy sources; smart grid

1. Introduction

Distributed energy resources (DERs) in various forms are rapidly being added to the electrical power grid. Most DERs are in the form of renewable energy sources (RES). Power electronic inverters are usually used as the interface between a RES and the power grid. DERs, or with some small difference in meaning, distributed generators (DGs) interfaced to the power grid with power electronic inverters are called inverter-based generators (IBGs), or sometimes more generally are called inverter-based resources (IBRs). To make DERs controllable, they are put in the form of microgrids (MGs), which are defined by the International Council on Large Electrical Systems (CIGRE) as [1]:

"Microgrids are electricity distribution systems containing loads and distributed energy resources (such as distributed generators, storage devices, or controllable loads) that can be operated in a controlled, coordinated way either while connected to the main power network or while islanded."

Conventionally, most of the generators in a power system are synchronous generators (SGs). These types of generators have well-defined controllers, which easily control the flow of both real and reactive power. Also, an SG usually has a heavy rotor, which provides big inertia that prevents sudden changes in the speed of the rotor, and this eventually helps to maintain the stability of the power system when disturbances occur in a section of the system. IBGs, on the other hand, do not naturally provide inertia except if it is

made virtually. Although control schemes have been developed to control their active and reactive power; firstly, they cannot be controlled over a wide range that was the case for SGs, and secondly, they have an intermittent power output, which is almost continuously varying and is not exactly predictable. According to the report by the IEEE PES Task Force on Microgrid Stability Analysis and Modeling [2], though having a generating unit close to the load in an MG helps in the reduction of voltage drop, the limitation on the output current of IBRs is a crucial factor for voltage instability of MGs. A Microgrid generates dynamics that impact the direction of the current flow and its magnitude [3]. Furthermore, the short-circuit capacity of an IBG compared to an SG is very low, which may cause a considerable drop in the MG fault level [4,5]. The low short-circuit capacity also limits its ability in providing the inrush current for induction motors [2,6], and creates a bus with lower strength compared with a similar bus connected to an SG.

These characteristics of IBGs cause some significant changes in the system characteristics concerning the power system stability and in particular the voltage stability [7]. To address these changes, various operation and control schemes have been proposed for power IBGs, for example [8–12].

The stability concepts and practices used for the conventional power systems are not sufficient for the stability analysis of MGs and power systems with a high level of connected DGs. The research has been conducted to develop new approaches for the stability analysis of systems with MGs. In the literature, two main approaches can be observed [13]: (a) small-signal stability assessments, and (b) investigating dynamics of the inverters.

2. Voltage Stability of Microgrids

Microgrids are managed autonomously, and act as either consumers or generators from both grid and market perspectives [14]. Microgrids can isolate themselves from the main power network in case of a fault or large disturbance [15,16]. The disconnection or reconnection is done through a single point of connection to the utility known as the point of common coupling (PCC). A microgrid must meet the established interface and interoperation requirements at the PCC, such as the one defined in the IEEE Standard 1547 for connecting inverters [17]. A microgrid integrated with the main grid presents several challenges in terms of electric grid operation and system reliability maintenance. Voltage stability in a microgrid can be defined as its ability to retain the buses/feeders' voltage level within an acceptable range during normal operating conditions as well as after any contingency event. Voltage instability is initially a local phenomenon and starts with an imbalance of reactive power. A sudden change in loads or a sudden change in load flow capacity like tripping of a transmission line are the two major causes of voltage instability. Keeping the voltage stable is one of the crucial aspects of microgrid operation and control, as the relatively low voltage levels, uncompensated loads, and current-limited inverter operation in microgrids put the network at risk for voltage instability and collapse [2]. In a system with voltage instability, there is at least one bus or feeder in the system for which the voltage magnitude (V) decreases with the increment of the reactive power injection (Q) at the same bus or feeder, i.e., dV/dQ is negative. In other words, a microgrid integrated system is voltage unstable if V-Q sensitivity is negative for at least one bus/feeder. Microgrid voltage stability phenomenon is broadly classified based on disturbances in the system; however, it can be further classified based on various other factors: whether the microgrid operates grid-connected or islanded; whether the study is about the DC-link voltage stability or it is about the system voltage stability; whether the system response to a small disturbance is examined or its response to large disturbance; and all other factors that affect the microgrid voltage stability such as the Q-V droop sensitivity, the inverter dynamics, load dynamics, and dynamics of other components, e.g., under load transformers tap changers. Figure 1 shows some of these classifications and the corresponding factors.
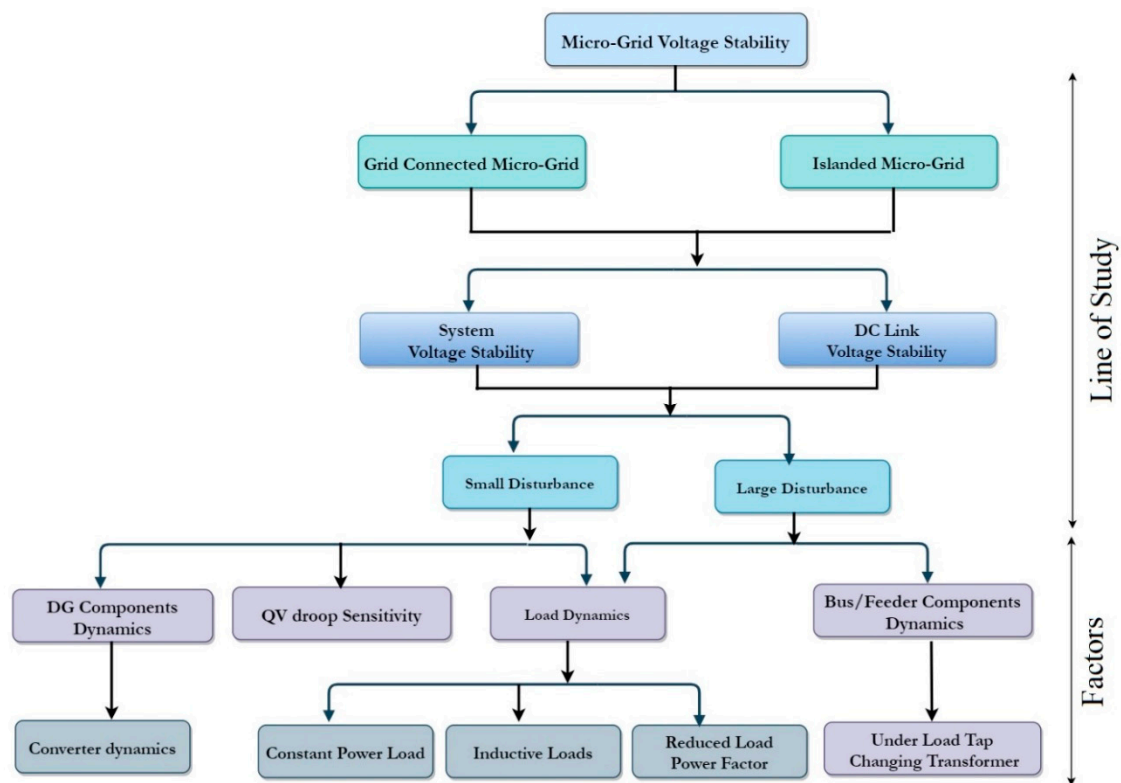
Figure 1. Study line for voltage stability in microgrids.

Islanded MGs with the domination of IBGs in their generator mix can be more vulnerable to disturbances than conventional power grids. Static voltage stability analysis is usually not sufficient for MGs [18]. It is obvious that to be effective in enhancing voltage stability, IBGs should have active and reactive power control to support the system. Many voltage support strategies for grid-connected IBGs have been reported in the literature, such as [19–22]. Enhancing voltage stability of islanded MGs with voltage support is reported in [23,24]. To mitigate the voltage instability of islanded MGs, prioritized reactive current injection from the inverter has been presented as a means for voltage support. Since islanded MGs contain considerable resistive line parameters [25,26], a sufficient active current component is also required in conjunction with the reactive current to enhance the dynamic voltage stability. Based on this requirement, effective coordination between the active and reactive current components for an IBG has been proposed in [27].

2.1. Microgrid Configurations

A general criterion for a bus of a power grid to contribute towards voltage stability is to be a strong bus, i.e., having high strength, giving smaller voltage changes in response to any disturbance [28]. The PCC of an MG is generally classified as a weak junction; it has a low short-circuit level and limited frequency/voltage control capability. Therefore, the first point of study for microgrid voltage stability should consider the microgrid layout architecture. Microgrid topology has considerable impact on loadability and voltage stability. It should be noted that a meshed-networked microgrid has the highest loadability while a radial network has the lowest loadability and this fact should be considered when evaluating voltage stability of microgrids.

A grid-connected microgrid can be classified either as a parallel-connected microgrid (PCM) or a mixed parallel-series microgrid (MPSM), while an islanded microgrid can be a single or a set of series-interconnected microgrids (GSIM). A grid-connected microgrid is a part of a strong grid with a relatively large number of online synchronous machines. However, an islanded microgrid is generally a weak grid and has a higher sensitivity in voltage variations with changes in both active and reactive power, i.e., dV/dP and dV/dQ.

In isolated hybrid microgrids (HMGs), the AC DER units can operate in three modes PQ, PV, or droop. Likewise, DC DER units can also operate in three modes: constant P, constant V, or droop. MPSM and GSIM layouts have the benefit of the connections with other microgrids to overcome a disturbance and maintain local voltage stability while islanded microgrids have limited voltage support to sustain the voltage at all load buses within the desired operational limits [29,30]. Hence, from the viewpoint of the system voltage stability, MPSM (having interconnections with the main grid, but also among microgrids) is the most favorable layout followed by GSIM and then PCM [14]. Another grid-connected MG architecture is based on integrating IBRs by employing a solid-state transformer (SST) to asynchronously interface the microgrid with the main grid. The general concepts of the SST are addressed in [31]. In [13], a complex and realistic AC microgrid is investigated and the scenarios defined are intended to link the inertia of the SST-microgrid with a voltage stability issue.

A microgrid may also be categorized based on the type of the loads it is serving as an AC microgrid or a DC microgrid. Although the AC loads are the prominent type of loads in electrical systems, DC MGs have started attracting attention due to several advantages, including their direct inherent simple DC connectivity, improved efficiency with less power conversions and associated losses, and lack of reactive power complexity [32,33]. A particular topology of interest is a DC microgrid connected to an AC grid. Reference [34] presents a qualitative comparison analysis of power management systems for grid-connected DC MGs. A seamless interchange method between interconnected and islanded mode of a DC MG is presented in [35]. A feasible power flow solution of DC MGs and analysis of existence of the feasible power flow solution of the DC MG under droop control is presented in [36]. The large-signal stability analysis of a DC MG from a system-level perspective is presented in [37] based on the Lyapunov method. In [38], a seamless disconnection of DC MGs from upstream power grid is presented. In its proposal, during normal operation the proposed controller allows power flow regulation at the converters' output. On the other hand, during abnormal operation of the grid-interface converter (e.g., due to faults in the upstream grid), the controller allows bus voltage regulation by droop control. The controller can autonomously convert from power flow control to droop control, without any need of bus voltage variation detection schemes or communication with other microgrid components, which enables seamless transitions between these two modes of operation. In [39], DC MGs are used as Virtual Synchronous Machines (VSM) connected to the AC grid. An autonomous integration concept for DC microgrids into the AC grid is proposed based on the VSM concept. It utilizes a DC–AC converter as a universal VSM-based interface (VSMBI) between the AC grid and various DERs connected on the DC side. A review on protection of DC MGs is presented in [40]. The paper also points out the key areas of future research in the protection of DC MGs, which lies in the development of novel protection devices based on electronic technology to provide loose protection constraints and the improvement of suitable protection schemes. In addition, the concept of coordinated strategy of control and protection of the DC MGs is explained.

Control of DC MGs and their load sharing are other active research areas. DC MGs are controlled for two main objectives: regulating the DC-link voltage to maintain the power balance between the sources and loads under steady state, and controlling dynamic conditions, which is a key for the reliable and stable operation of DC MG and load sharing while in the isolation mode [41]. Appropriate load sharing approaches are used to distribute the loads in proportion to rated power of the participant converters, which reduce the stress on each source and prevent the circulating currents [42]. However, unlike in an AC MG, loads in a DC MG, if not controlled, are distributed among sources/converters based on the resistances of the cables connecting converters to loads, and not based on the rating of the converters. The most widely implemented methods for sharing loads are the droop-based control methods, in which load sharing is achieved by adding a virtual resistance control loop as an external loop for the converter's voltage control loop to facilitate sharing of the currents. The main advantage of droop-based control methods is its simplicity and

ease of use. However, its accuracy is affected by voltage deviations due to dynamics of the loads and resistances of the power lines [43]. In addition, while droop control in its basic form can be implemented locally without any communications infrastructure [32], the accuracy of load sharing can be highly inaccurate without any communication link. This limits the viability of this approach. In order to improve the load sharing accuracy, centralized approaches based on communication networks were proposed.

2.2. Interlinking Converters, DC-Link Voltage, and Islanded Microgrids

The DC-link and interlinking converters (ICs) are key elements for coupling DGs into a microgrid. In an AC grid, active power flow is proportional to the voltage angle, as shown in Equation (1).

$$P = \frac{V_S V_R}{X_{AC}} \sin \delta \qquad (1)$$

where V_S is the sending-end voltage, V_R is the receiving-end voltage, and X_{AC} is the line reactance. Frequency is proportional to δ, hence frequency can be controlled by the active power or vice versa.

In a DC grid, the active power flow is proportional to the DC voltage (V_{DC}), as shown in Equation (2). Therefore, the DC link voltage can be controlled by the power and vice versa.

$$P = V_{DC} \frac{\Delta V_{DC}}{R_{DC}} \qquad (2)$$

where ΔV_{DC} is the voltage drop over the line resistance R_{DC}.

The control system of a DC microgrid is considerably simpler than an AC microgrid due to the absence of control complexity for angular and frequency stability. Each AC DER unit is associated with four quantities: the magnitude of the AC terminal voltage $|Vac|$; the phase angle δ; the active power output P_{DR}; and the reactive power output Q_{Dr}. In contrast, each DC DER unit is related to only two quantities: the DC terminal voltage, V_{Dc}, and the active power output. The autonomous control of various parallel-connected converters can be easily realized through a DC bus signal control method where different voltage levels represent different operating states [44]. Stabilization of the DC-link voltage is also an important factor for maintaining microgrid dispatchability. Increasing the load in a DC microgrid decreases the voltage across the DC link capacitor, which may affect the voltage stability margin of the microgrid network. Therefore, as a common design criterion, droop control is implemented with the largest droop coefficient, while limiting the DC voltage deviation at the maximum load condition [45]. Besides normal droop control, non-linear and adaptive droop control were also researched to achieve acceptable voltage regulation at full load [46–48]. However, these methods suffer from poor voltage regulation especially when line impedance are non-negligible. Hence, the remaining voltage deviation is then eliminated by implementing secondary control to achieve global voltage regulation, as was stated earlier.

Various DGs integrated into a DC microgrid act as dispatchable and non-dispatchable units. Non-dispatchable DGs interface with the microgrid through conventional current-driven interfacing inverters, while the interaction between the microgrid and the utility at their PCC happens via a voltage-driven grid-interactive inverter. Since dispatchable units are mainly responsible for stabilizing the voltage of the DC microgrid, grid forming ICs operating as constant voltage sources employ outer voltage control loops and inner current loops to stabilize the DC-link voltage to a set reference voltage [49]. Non-dispatchable energy units are mainly responsible for maintaining constant power output. Some other dispatchable units also work in the constant current mode. Their corresponding ICs are known as grid-feeding converters and also require DC-link voltage as one of the signals in its constant current control loop [49]. The control loops concept for grid-forming and grid-feeding converters are shown in Figure 2.
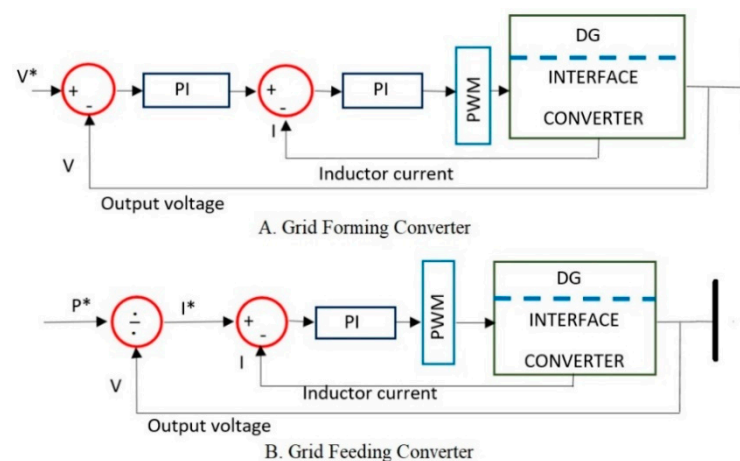
Figure 2. Control loops for grid-forming and grid-feeding converters [49].

Microgrids require primary and secondary voltage control when operating in the islanded mode, while tertiary voltage control is also effective during their operation in the grid-connected mode.

In grid-connected mode, the grid normally absorbs all the power generated by IC in a microgrid. However, in the cases of grid loss, each inverter should receive, from a supervisory controller, new settings of the output power suitable to the microgrid load. However, slow-acting supervisory control may lead to significant DC link voltage rise due to the excess of circulating power among the ICs during low load [50]. A voltage support strategy for grid feeding converter with new coordination between the active and reactive current injection considering the voltage level as well as the margin residue is proposed in [26] to improve the dynamic voltage stability of the islanded microgrid. Margin residue is introduced in this strategy to avoid any damage in the inverter due to the over current flow more than the maximum current. Voltage stability within acceptable limits can also be assured through proper design and implementation of ICs in an islanded hybrid MG. Microgrid loadability during contingency can be balanced by interfacing with an adjacent microgrid. In islanded AC–DC hybrid microgrids (HMG), the amount and direction of power transfer is realized through a droop characteristic implemented by the IC. The IC interfacing autonomous AC and DC subgrids always consider the loadability of both subgrids by measuring the frequency of AC grid and voltage of DC grid. The normalized frequency and normalized DC voltage are then utilized to determine the droop characteristic of HMG [41,51]. In an islanded HMG, IC changes the operating role based on power transfer direction. It is seen as a current source by heavily loaded subgrid or as a load for lightly loaded subgrid. When operating in grid-forming mode or voltage-controlled mode, ICs share the responsibility of maintaining the voltage with other DGs while if IC cannot control the voltage at its AC terminal, it switches to the current-control mode to operate in the grid supporting mode.

2.3. The Effect of Size and Duration of Disturbance

Another line of study for the microgrid voltage stability can be classified in terms of size and duration of disturbances, and the physical nature of voltage instability [52]. There may be different factors leading to various forms of disturbances resulting in voltage instability problems. Large disturbance voltage stability is concerned with the system's capability to regulate bus/feeder voltages following large and long-term contingencies beyond the normal system design criteria like a large fault or a generation loss. Small disturbance voltage stability is related to minor system perturbations like demand changes [23]. As the size of a microgrid is very small compared to the power grid, a microgrid in grid-connected mode operates like a controllable load/source. However, system dynamics have to be controlled and fixed to a wide extent [17]. Long-term voltage instability can occur in systems with heavy loads like islanded MPSM where there is a long electrical distance

between the generator and the load. Large disturbance stability analysis over the long term necessitates the investigation of dynamic interactions of power line characteristics, tap changing transformer operation, and load dynamics. On the other hand, small disturbance voltage stability analysis is investigated for the load dynamics and system control methodology for governing V-Q sensitivity. A network with $X \gg R$ is usually stable where $\frac{dQ}{dV}$ is positive.

2.4. The Effect of Load Dynamics

Besides disturbances in the network, load dynamics affect the voltage instability. Load dynamics depend upon several parameters such as the power factor or variation of active and reactive power flows with voltage and frequency. Usually, a microgrid with a constant-impedance static load has stable dynamics. Conversely, a microgrid with a constant-power load (CPL) may become unstable due to incremental negative impedance, which may result in the collapse of the load bus voltage. Many loads like motor drives or electronic loads with closed-loop power electronic converters behave as CPLs. On the other hand, the open-loop converter behaves like a resistive load [53]. During a small disturbance, the load current increases to keep the constant power output and at the same time, the load voltage will decrease. In case of an improper converter control, the load voltage may drop to very small values close to zero and may lead to complete voltage collapse [54]. Fault-induced delayed voltage recovery (FIDVR) is also a factor in the voltage stability of microgrids having high penetration of inductive loads. Induction motors under stalling condition may absorb up to three times their nominal reactive power to re-magnetize. The insufficient reactive power supply in such cases leads to system voltage instability. An effective strategy to improve voltage stability in a microgrid with multi-induction motor (MIM) loads was proposed by applying methods of superimposed starting strategy and fast motor cutting strategy [55].

Even though load shedding is proposed in many cases to improve the dynamic voltage stability, it is not a desirable solution in many cases. If the loads are supplied by transformers with automatic under load tap-changing (ULTC), when the voltage decreases, the tap-changer action will try to raise the load voltage. This effectively reduces the impedance as seen from the system. This in turn can lower the voltage regulation and may lead to a progressive reduction of the voltage, which in some conditions may eventually move towards a voltage collapse.

For a constant sending-end voltage, a sudden reduction in the receiving-end load lagging power factor (i.e., an increase in receiving-end load reactive power) can cause the system to change from a stable operating condition to an unsatisfactory and possibly unstable operating condition [56], as shown in the P-V curve in Figure 3, with comparison of the curve related to cos φ = 1.0 with the curve related to cos φ = 0.95 lag.
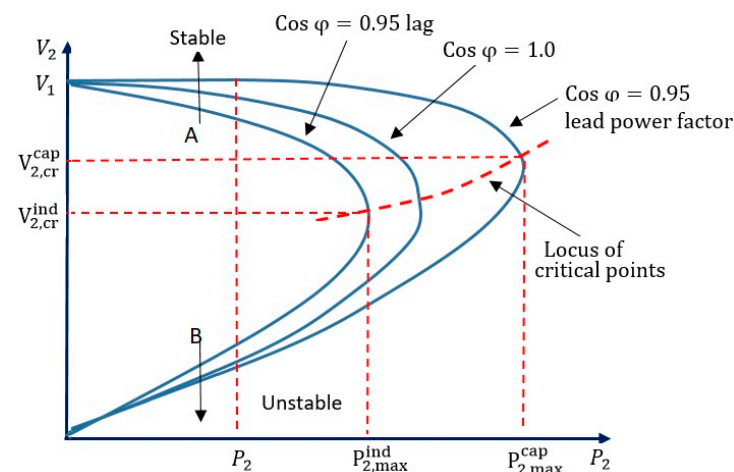

Figure 3. Effect of reactive power compensation on the P-V characteristic.

The penetration of DG units in a microgrid can increase or decrease the voltage stability margin depending on their power factors as well as their locations. For the long-term voltage stability, it is more beneficial to have DGs operating at generating lagging power factors to improve the voltage security margin, i.e., increasing the distance to voltage collapse. When a DG operates at a leading power factor, the short-term voltage stability is generally improved as the voltage dips are reduced.

2.5. Coordination of Voltage Control Loops

Reactive power is generally supplied for improving the bus/feeder voltage profile during short-term faults. In islanded microgrid clusters, where generating units are nearby and feeder lengths are relatively short, it is easy to achieve desired reactive power-sharing by manipulating voltage control associated with DGs. Any variations in the terminal voltages of DGs are almost closely reflected in the rest of the MG buses or feeders [57]. In practice, proper reactive power-sharing among multiple DERs in a microgrid is most commonly done through the DG interfaced converter's Q-V droop control loop. Voltage stability can be improved by adding DC links among radial feeders. But, AC/DC loops change the network topology from radial to mesh, thus making its operation and control more difficult [58]. Appropriate coordination of Q-V droops is crucial to avoid high circulating reactive power flows, which may result in large voltage oscillations [59]. Conventional Q-V droop control in islanded microgrid suffers from limitations such as poor voltage regulation due to the inappropriate reactive power sharing due to line impedance mismatch and non-identical bus voltages. There is a linear reduction in the magnitude of the reference output voltage of a DG with the increase in the injection of its reactive power [60]. Thus, DGs with steeper Q-V droop slopes may present poor dynamic performance especially in the presence of non-linear loads. Higher droop gains in the primary control can reduce the effect of line resistances on the current sharing accuracy, but also can cause large voltage drops in the output terminal of the converters [49]. Furthermore, during overloading and islanding conditions, DGs with voltage support capability may have to operate near their limits [58]. Some of these DGs could reach their limits due to a subsequent contingency. In such a situation, they normally switch to the current-control mode. As a consequence, the entire microgrid could lose voltage control and eventually collapse.

Considering current mismatches and voltage drops caused by primary droop control, a secondary controller is needed for maintaining voltage stability in the microgrid. Centralized approaches such as hierarchical control and distributed control approaches have been proposed as an alternative to improve the load sharing accuracy (e.g., [12,32]). The secondary controller measures the DC-link voltage, calculates the voltage correction factor, and provides it to all converters in the microgrid to increase their output voltages.

A centralized hierarchical primary-secondary voltage control scheme for maintaining the DC-link voltage at only one bus/feeder/PCC of a microgrid is presented in Figure 4, where R_d represents the droop setting, R_1 is the line resistance, V^* is the rated DC-link voltage, V_{MG} is the measured DC-link voltage, and δV is the calculated voltage correction factor. In the hierarchical control approach, an additional control layer is added (secondary control) to communicate with the primary droop control. The secondary control sets the parameters for the primary control. In the distributed control approach, instead of using single secondary control, distributed controllers are implemented in each of the participating converters. These controllers communicate among each other using a common bus [61]. This approach normally ensures accurate load sharing and better voltage regulation as compared to that of hierarchical control.

Various decentralized secondary controllers are presented in the literature for maintaining voltage stability at different buses/feeders in a microgrid network. A consensus global average voltage estimator-based distributed secondary controller is discussed for average voltage stability maintenance of the grid-supporting buses; however, this scheme is not applicable for load buses in a microgrid network [62].
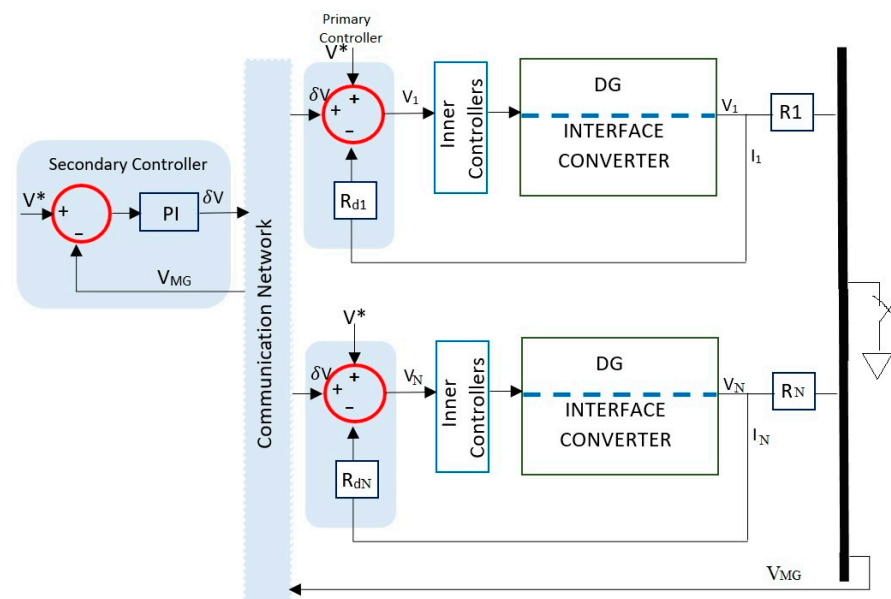
Figure 4. The hierarchical primary-secondary voltage control scheme for a DC microgrid [49].

2.6. Methods of Analysis for Determining Voltage Stability in Microgrids

The vulnerable sections of the network may be identified through appropriate voltage stability assessment methods. Selecting a suitable method for voltage stability analysis of a network depends on mainly two aspects of the problem: (a) proximity to voltage instability, and, (b) mechanism of voltage stability [52]. Appropriate mitigation methods can then be applied to enhance the stability of the network. Voltage stability in general can be evaluated by two different methods of analysis, static and dynamic, as presented in Figure 5.
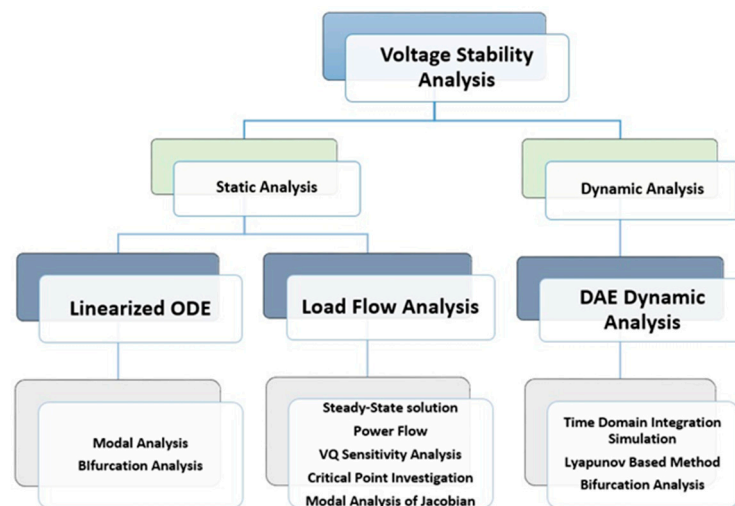

Figure 5. Voltage stability analysis in microgrids.

System dynamics that influence voltage stability are usually slow. Therefore, voltage stability analysis can be done by using some selected static operating conditions of the power system. The static analysis techniques can highlight the nature of the problem related to voltage stability and identify the key contributing factors. Dynamic analysis, on the other hand, is useful for detailed study of specific voltage collapse situations, coordination of protection and controls, and testing of remedial measures.

2.6.1. Static Voltage Analysis

(a)   P-V and Q-V Curves

An electric power grid can be represented by three distinct quasi-steady-state characteristics for the three stages of the disturbance: pre-disturbance, post-disturbance, and post-disturbance with reactive power support. In Figure 6, a network operates in normal conditions at a point lying at the intersection of the pre-disturbance characteristic and the steady-state load characteristic $Q_d(v)$. Following a disturbance, the network's reactive power capability is reduced, and the operating characteristic jumps to point b of the post-disturbance characteristic, as shown in Figure 6.
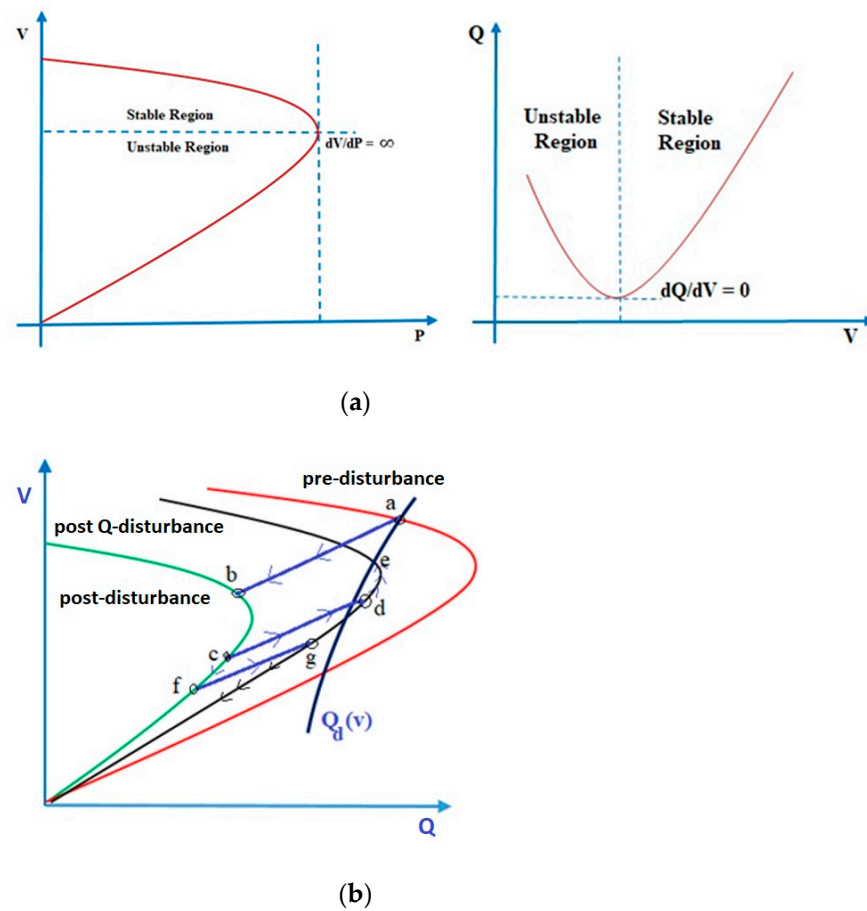

(a)

(b)

Figure 6. (**a**) P-V and Q-V Characteristics, (**b**) Q-V characteristics for pre-and post- disturbances [39].

The network voltage will reduce to reinstate the reactive power and the corresponding transient load dynamics can be expressed as:

$$Q_d(v) = \gamma V^\beta \tag{3}$$

Here, γ is the state variable. $\beta = 2$ when the load is modeled as an impedance, whereas $\beta = 1$ if the load is modeled as a current [56]. The voltage will continue to reduce monotonically till the reactive power supply $Q_s(v)$ is less than the reactive power demand $Q_d(v)$, and the operating point moves from point b to point c or further to point f. With the external reactive power support, the post-Q support operating point jumps from point c to point d where the voltage begins to increase until the operating point reaches an equilibrium, at point e. P-V and Q-V curves are generated by executing a large number of

power flow using continuous power flow methods. An electric network can be typically modeled with non-linear differential-algebraic equations as indicated below [63].

$$x = \dot{f}(x, \lambda) \tag{4}$$

where $x \in R^n$ represents a state vector, including the bus voltage magnitude (V) and angles (δ), and $\lambda \in R^m$ is a parameter vector that represents the real and reactive power demand at each load bus. The parameter vector λ is subject to variations due to variations in the load. Therefore, the power flow solution varies as λ varies. It is ideal to operate the network node farthest from the P-V critical point $\lambda_{\max}$, which represents the maximum loading of the network. A high load impedance is required in comparison to the equivalent network seen at the node to have stronger voltage/load stability and a superior voltage profile.

(b)   bV-Q sensitivity analysis

In this modal analysis method, the network is represented by a power flow equation that can be linearized [64]. The voltage characteristics of a power system are analyzed around an operating point by linearizing the power flow equations and analyzing the resulting sensitivity matrices. The element in the matrix is calculated by the relative relationship between the state variables as shown by the following equation.

$$\begin{bmatrix} \Delta P \\ \Delta Q \end{bmatrix} = \begin{bmatrix} J_{P\theta} & J_{PV} \\ J_{Q\theta} & J_{QV} \end{bmatrix} \begin{bmatrix} \Delta\theta \\ \Delta V \end{bmatrix} \tag{5}$$

where

ΔP is the incremental change in the bus real power,
ΔQ is the incremental change in the bus reactive power,
ΔV is the incremental change in the bus voltage magnitude,
$\Delta\theta$ is the incremental change in the bus voltage angle,
J is the Jacobian matrix.

With the assumption of the real load power (P) being constant, the incremental change in the bus real power ΔP equals zero. Then, using the partial inversion of Equation (5) gives:

$$\Delta Q = \left(J_{QV} - J_{Q\theta} J_{P\theta}^{-1} J_{PV} \right) \Delta V \tag{6}$$

or

$$\Delta V = \left(J_{QV} - J_{Q\theta} J_{P\theta}^{-1} J_{PV} \right)^{-1} \Delta Q \tag{7}$$

The V-Q sensitivity can be calculated by solving the above equations. A positive V-Q sensitivity is an indication of stable operation, while a negative sensitivity indicates unstable operation [52].

(c)   QV modal analysis

Voltage stability can be analyzed by calculating a certain number of the left and right eigenvalues and associated diagonal eigenvalue matrix of the reduced Jacobian matrix [65].

$$J_R = \left(J_{QV} - J_{Q\theta} J_{P\theta}^{-1} J_{PV} \right)^{-1} \tag{8}$$

The magnitude of the eigenvalues associated with a mode of a voltage/reactive power change provides a relative measure of proximity to voltage instability. The eigenvalues of the matrix also indicate different modes in which the voltage instability may occur in the system. Each eigenvalue and the corresponding right and left eigenvectors define the ith mode of the Q-V response. For the ith mode:

$$v_i = \frac{1}{\lambda_i} q_i \tag{9}$$

If $\lambda_i > 0$, the system is voltage stable. If $\lambda_i < 0$, the system is voltage unstable. The magnitude of λ_i determines the degree of stability of the ith modal voltage. The smaller the magnitude of positive λ_i, the closer the modal voltage to being unstable.

2.6.2. Dynamic Analysis

Microgrids with their highly time-varying and non-linear components require specialized voltage stability techniques accounting for the effects of long-term higher-order dynamics. Both short-term and long-term voltage stability evaluations are performed with time-domain dynamic simulations involving dynamic models of generators, loads, and other components of the microgrid network. Dynamic analysis can show the real behavior of the system components such as loads, DG units, automatic voltage and frequency control equipment, and protection systems. The power electronic converter used for the DG integration contains control loops and algorithms with very fast response time. In dynamic analysis, the whole network is represented by a set of differential-algebraic equations (DAEs), as given by [66]:

$$\dot{x} = f(x, V) \tag{10}$$

and a set of algebraic equations:

$$I(x, V) = Y_N V \tag{11}$$

along with a set of known initial conditions (X_0, V_o).

Here, x is the state vector of the system,

V is the bus voltage vector,

I is the current injection vector, and

Y_N is the network node admittance matrix.

Equations (10) and (11) can be solved in a time domain using numerical integration methods or power flow methods with sufficiently low time steps taking several minutes.

(a)   Microgrid voltage stability analysis through time-domain power flow simulations

Most of the voltage stability analysis tools are based on the power flow equations or their modifications. However, for islanded microgrids, since it is required to incorporate the hierarchical control effects for the power flow analysis, it becomes a challenging problem. The mathematical model based on the differential and algebraic equations are initially solved through the power flow algorithms; however, more states and algebraic variables are involved to build models for a microgrid. In a traditional Backward/Forward Sweep (BFS) power flow, there is one swing bus and all others are PQ buses or PV buses. But, in islanded microgrids, there is no swing bus to balance the power loss and the power gap caused by islanding. Instead, it is shared among all DGs according to the control mode. A generalized microgrid power flow (GMPF) incorporating a generalized DG bus and an adaptive swing bus to model the behavior of DGs is devised in [67] to incorporate hierarchical control. GMPF is initialized through the power flow results of a droop-based microgrid. A dummy bus virtual impedance is utilized for Q-V sensitivity. The power flow problem for islanded microgrids can be defined by a set of time-domain nonlinear equations, which can be solved as an unconstrained minimization problem [68]. The hybrid microgrid power flow problem can be solved through a computational approach like a sequential Newton Raphson-based power flow algorithm [69] or unified approach [70]. In the sequential method, the AC and DC power flow sub-problems are solved iteratively and sequentially until the sequential power flow algorithm converges while in the unified AC/DC hybrid power flow program, the AC and DC power flow subproblems are solved simultaneously for obtaining a minimum solution defined as follows [71].

$$\underset{x \in R^n}{\text{minimize}} \quad f(x), \ f : R^n \to R^n \tag{12}$$

where

$$f(x) = [f_{ac}(x_{ac}), f_{dc}(x_{dc})]^T, \quad x = [x_{ac}, x_{dc}]^T \tag{13}$$

with $f(x)$ as the vector of the equations describing the power flow problems in the AC and DC microgrids, and x as the vector of the AC/DC control (independent) and state (dependent) variables. The following equation gives the kth iteration of $f(x)$:

$$f\left(x^{(k)}\right) = -J\left(x^{(k)}\right)\Delta x^{(k)} \tag{14}$$

where $J\left(x^{(k)}\right)$ is the Jacobian matrix at iteration k for AC and DC sub-grids.

(b)   Voltage stability analysis through Lyapunov-based assessment method

Lyapunov stability is one of the dynamic analysis methods to discuss the solutions of differential equations based on the switched microgrid model. A switched system is asymptotically stable if the eigenvalues of its state transition matrix have negative real parts. For a switched linear system, there exists a positive definite symmetric matrix Q for which a unique positive definite symmetric matrix P satisfies the Lyapunov equation as given below:

$$A_P^T P + P A_P \leq -Q, \tag{15}$$

In [72], based on control theory, a framework for studying voltage stability in distribution systems composed of networked microgrids was presented. The framework involves non-linear state-space modeling of the microgrid components including loads and generators as nodes and the network connections as a set of topology-based algebraic equations. The networked system consists of a main grid connecting point and n microgrid nodes. This state-space model for the entire network of microgrids may be viewed as a closed-loop system. Based on the Lyapunov stability of the closed-loop systems, all eigenvalues of Jacobian J must be in the open left-half plane. It was shown that the voltage stability for a resistive network of a radial topology at the equilibrium point can be determined by the eigenvalues of $J(P0)$, where $P0$ belongs to the stable region. Here, P is the target power consumptions for the loads. The voltage regulation of a three-phase islanded microgrid is discussed in [73] using a direct-Lyapunov-based control scheme. The inner local controller for each DG unit is derived based on the direct Lyapunov stability theory.

(c)   Bifurcation analysis for voltage stability study of microgrids

The bifurcation phenomenon happens with continuous but small changes in one or more parameters leading to a sudden change in the system stability. Hopf bifurcation and saddle nodal bifurcation (SNB) are the main bifurcation phenomena in power systems. In the case of Hopf bifurcations, a pair of complex conjugate eigenvalues are on the imaginary axis resulting in sustained oscillations appearing in the power system due to stability loss. An SNB of a power system operation state is defined as a point at which two power flow solutions merge, then disappear as the load active power is slowly increased. During an SNB, a real eigenvalue is located on the imaginary axis and the system stability is completely lost with continuous parameter variations. The SNB is the loading point at which the voltage collapses and is used in operational planning. An SNB bifurcation analysis on the P-V plane of islanded microgrid was undertaken in [74].

Under the influence of a virtual inductor, the PCC voltage was observed to be decreasing very fast when an induction motor (IM) load or a constant power load was close to the SNB boundary, suggesting voltage instability. The bifurcation phenomena do not exist for the PV curves of constant-impedance and constant-current loads as shown in Figure 7. For a small reduction in nominal voltage, the SNB analysis confirmed the shrinkage of the stable range of load assumptions.
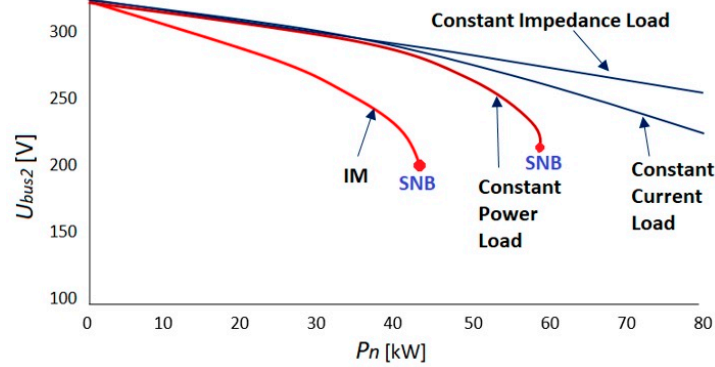
Figure 7. Saddle nodal bifurcation (SNB) phenomenon for the PV curve with increasing loads [74].

3. Voltage Stability Indices for Microgrids

Three key factors influence the voltage stability of a microgrid: (a) reactive power limits, (b) dynamics of loads, and (c) tap changing transformers [75]. Many voltage stability indices (VSIs) were derived in the literature to assess the stability of power grids. A comprehensive review of VSIs was presented in [76], mainly based on high voltage transmission systems. In the microgrid planning, voltage stability indices were used for the connection of DERs as these indices help to identify the weak bus or lines [77]. Furthermore, these voltage stability indices help to determine the proximity of the voltage collapse, voltage stability margin, loading conditions, voltage stability sensitive buses or lines, and reactive power requirements during the practical operation of microgrids [78]. The characteristics of microgrids are completely different from traditional power transmission systems, and as such, many of the traditional VSIs are obsolete for analyzing the voltage stability of microgrids. However, the majority of the existing VSIs can easily be modified by considering DERs in either the sending or receiving end of a two-bus circuit representing a part of a microgrid. This network is used to determine the indices. As indicated in [79], if DERs are connected to the receiving end, the active and reactive power at the receiving end can be calculated as:

$$P_r = (P_{DER} - P_L) \tag{16}$$

$$Q_r = (\pm Q_{DER} - Q_L \pm Q_C) \tag{17}$$

where P_{DER} and Q_{DER} are active and reactive power of DERs, respectively; P_L and Q_L are active and reactive power of DERs, respectively; and Q_C is the reactive power of the compensator. The reactive power of the DER and compensator can either be positive or negative depending on the situation. For example, the reactive power of a DER will be negative if an induction generator-based wind farm is used. Similarly, compensators were used to control the bus voltage and these will consume reactive power (i.e., Q_C will be negative) if there are voltage rises or vice-versa.

The fast voltage stability index (FVSI), as presented in [80], is the most commonly used voltage stability index and this needs to be modified as follows for the implementation in microgrids:

$$FVSI_{sr} = \frac{4Z_{sr}^2 Q_r X_{sr}}{V_s^2 (R_{sr}\sin\delta + X_{sr}\cos\delta)^2} \leq 1 \tag{18}$$

where Z_{sr} is the impedance between the sending and receiving end; X_{sr} is the reactance between the sending and receiving end; R_{sr} is the resistance between the sending and receiving end; δ is the difference of the voltage angles between the sending and receiving end, and V_s is the sending end voltage. The value of $FVSI_{sr}$ should always be less than one for maintaining the voltage stability in a microgrid and if its value is greater than one, the microgrid will experience a voltage drop where this can be controlled by regulating either DERs or reactive power compensator. These indices are also used in [81] to rank line outages for the voltage stability assessment.

The line stability indices can be calculated by considering the effects of only active or reactive power [82,83]. These indices are generally derived from the fundamental voltage and power relationships. The line stability index by considering only the effect of reactive power can be written as [82]:

$$L_Q = \frac{4X_{sr}Q_r}{V_s^2(\sin(\theta - \delta))^2} \leq 1 \tag{19}$$

Similarly, the line stability index by considering only the effect of active power can be written as [83]:

$$L_P = \frac{4R_{sr}P_r}{V_s^2(\cos(\theta - \delta))^2} \leq 1 \tag{20}$$

where θ is the impedance angle. For the stable operation, the values of L_Q and L_p should be less than one. These indices are known as the line voltage stability indices [84]. The index L_p is also termed as the power stability index (PSI). For transmission systems, these stability indices (i.e., $FVSI_{sr}$, L_Q, and L_p) are calculated by using $\delta = 0$, but this is not done for microgrids.

Another important voltage stability index is the voltage collapse proximity index (VCPI) and several studies are carried out to determine this index, which can be found in [85,86]. The VCPI in [85] is obtained by considering maximum loading conditions in the transmission system while the power transmission paths are considered in [86]. A novel line stability index (NLSI) is calculated in [87] based on the formula derived for the FVSI with some assumptions. Several other indices have been introduced for transmission systems. A new voltage stability index was proposed in [88]. Other VSIs include voltage reactive power index (VQI) [89], voltage stability load index (VSLI) [90], voltage stability index [91] or indicator (VSI) [92], voltage stability margin (VSM) [93], VSM index (VSMI) [94], stability index (SI) [95], line collapse proximity index (LCPI) [95], and power transfer stability index (PSTI) [96]. However, these cannot be directly employed for microgrids, and need to be modified. All these stability indices are usually determined based on $FVSI_{sr}$, L_Q, and L_P with different assumptions where these assumptions include the following:

- Zero resistance of the line, i.e., $R_{sr} = 0$;
- No angle difference between the sending and receiving end, i.e., $\delta = 0$;
- No DERs at either sending or receiving end, i.e., $P_G = 0$ and $Q_G = 0$; and
- No shunt admittance.

All these assumptions are not feasible for microgrids and hence, thus these indices cannot be used directly. These stability indices are categorized as the line voltage stability indices in [76].

Apart from line voltage stability indices, different bus voltage stability indices are also reviewed in [76]. In [97], a voltage stability evaluation index called the voltage collapse proximity index (VCPI) is defined as:

$$VCPI_i = \left| 1 - \frac{\sum_{\substack{j=1 \\ j \neq i}}^{N} V_j'}{V_i} \right| \tag{21}$$

where $VCPI_i$ is the VCPI for bus i, V_i is the voltage of bus i, and $V_j' = \dfrac{Y_{ij}}{\sum_{\substack{k=1 \\ k \neq i}}^{N} Y_{ik}} V_j =$

$\left| V_j' \right| \angle (\delta_j')$ with Y_{ij} as the admittance between bus i and bus j. In determining VCPI, the voltage magnitudes and angles of all buses are used plus the network bus admittance

matrix information. A value of VCPI close to 0 indicates stability and a value close to 1 indicates approach towards voltage collapse. This VCPI is used in [98] along with two other indices, namely a voltage security index (VSI) and a power transfer stability index (PTSI), for the assessment of voltage stability in microgrids, and to particularly send signals to the microgrid control center when the dynamic state of the power system is not acceptable. The concept of power flow study is used to determine several bus voltage stability indices for transmission systems and these methods are *L*-index [99], voltage stability index using voltage and current deviations [100], simplified voltage stability index [101], and *S* difference criteria [102]. In [103], the bus voltage stability index is calculated based on the impedance matching, while in [104], the impedance ratio is used to determine the similarity index. All these indices are developed with assumptions related to the topology of the system, efficiency of the system, and eliminating the incremental changes in the power at the receiving end.

3.1. Impact of Load Variations on Voltage Stability Indices

Voltage stability indices are sensitive to loading variations and must present a predictable behavior by allowing extrapolation of the additional power requirement by the network before moving to the voltage instability point. It must be noted that the voltage stability indices can be monitored with the changes in system parameters, and their calculation must be fast enough for online system supervision feasibility. P-V curves are either calculated offline or estimated. Thevenin-based parameters offer an effective way to estimate P-V curves. The P-V method based on offline statistics cannot reliably predict voltage instability. Similarly, the Thevenin-based method relying on the measured parameters of aggregated loads has low accuracy.

3.1.1. Improved Thevenin Estimates

The interaction between the transmission and distribution system can cause the overall voltage stability margin to be different from the individual network. A 3φ voltage stability indicator incorporating the unbalances and coupling between the phases is proposed in [105]. The proposed voltage stability indicator is based on estimated Thevenin equivalent parameters through microphase measuring units (μPMUs). The ratio of the magnitude of the total apparent power loss and the total apparent load power is an indicator of voltage stability. This concept is extended to the three-phase (3φ) networks for the 3φ VSI, as given by Equation (16):

$$VSI_{D-3\varphi} = \frac{\left|S_{LossT-3\varphi} + S_{LossD-3\varphi}\right|}{\left|S_{LD-3\varphi}\right|} \tag{22}$$

where, $S_{LossT-3\varphi}$ is the apparent power loss at the transmission line side and $S_{LossD-3\varphi}$ is the apparent power loss at the distribution side, while $S_{LD-3\varphi}$ is the apparent load. For a balanced network and balanced load, the $VSI_{D-3\varphi}$ parameters are replaced by their positive sequence impedances, as shown in Equation (17).

$$VSI_{D-3ph-balanced} = \frac{|Z_{TP} + Z_{DP}|}{|Z_{LD}|} \tag{23}$$

Another new real-time voltage stability index S_I for a smart grid was proposed in [106]. The method utilizes the data of individual loads, which are obtained through the smart meters for estimating the Thevenin equivalent parameters.

$$S_I = 1 - sin\left(\frac{\pi D}{2}\right) \tag{24}$$

where

$$D = \sqrt{\frac{(P_{max} - P)}{P_{max}}} \tag{25}$$

$$P_{max} = S_{max}cos(\theta_L) \tag{26}$$

$$|S_{max}| = \frac{3|V_{th}|^2}{|Z_{th}|(2 + 2cos(\theta_{th} - \theta_L))} \tag{27}$$

3.1.2. Voltage Stability and Quality Index (VSQI) for PV-ESS Integrated Low Voltage Networks

Voltage stability and quality index (VSQI) for PV-ESS-integrated low voltage networks are presented in [107]. The VSQI is unique in terms of jointly capturing the voltage stability and voltage quality of the network having DGs and energy storage systems (ESS) complementing the power requirement. The voltage stability index was analyzed for different scenarios including network operation without ESSs utilization, and grid operation with ESSs powered by DGs. The VSQI can provide the assessment of the qualitative and secure operation of a future (e.g., next 10 min) operating state of the power system. The VSQI as given by Equation (28) is identified through the voltage stability triangle formulated out of the voltage stability curve as plotted between the voltage and stress factor of the network.

$$VSQI_\in = \sqrt{\left(x_\varepsilon^{vs} - x_\varepsilon^{vq}\right)^2 + \left(y_\varepsilon^{vs} - y_\varepsilon^{vq}\right)^2}, \quad \varepsilon \in [01] \ or \ \varepsilon \in [03] \tag{28}$$

The stress factor (k) is related to the network loading in terms of the increment in active and reactive power requirements. For any non-negative value of k, sequential power sweeps were performed to obtain the voltage stability curve. For various scenarios, the peak of the triangle as shown in Figure 8 is related to the voltage stability (vs) and voltage quality (vq) parameters, respectively. (x_0^{vs}, y_0^{vs}) denote the vq and vs for the network operation without the grid support units (0), while (x_1^{vq}, y_1^{vq}) denote the *vq* and *vs* for the network operation with the ESS supporting the network operation (1).
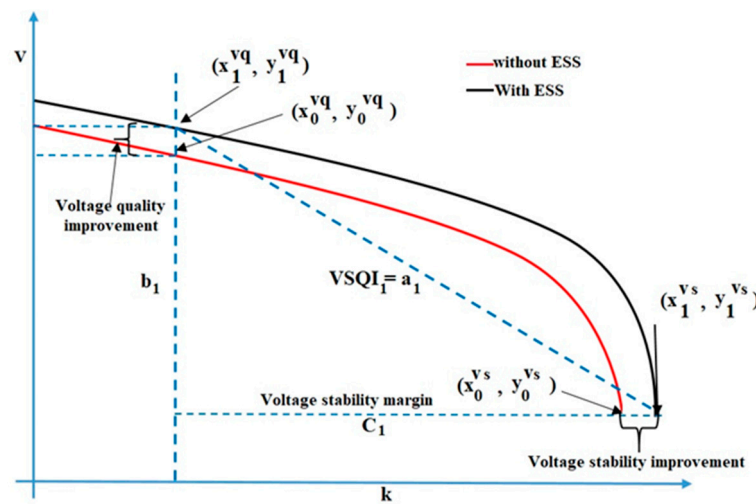

Figure 8. Voltage stability and quality index (VSQI) formulation from voltage stability curves [107].

For a community level ESS, ε belongs to [01], with 0 representing the no grid support and 1 indicating the operation of a community level ESS. $\varepsilon \in [0\ 3]$ represents the case when more than one ESSs provide support to the grid operation. Here, $\varepsilon = 1$ shows that only one of the three ESSs is operational. When the first and the second ESSs operate together, then $\varepsilon = 2$, and finally when all the three ESSs are dispatched then $\varepsilon = 3$. A significant improvement in voltage stability and quality was noted through the higher value of VSQI with increased power injection from the ESSs. Further better voltage stability was observed with larger concentrated ESS rather than distributed ESSs.

3.1.3. Hybrid Voltage Stability Margin (VSM) Index

To integrate distributed energy resources within distribution systems, probabilistic voltage estimation is required. In [108], a long-term voltage stability margin estimation based on artificial intelligence (AI) techniques that combines a Kernel Extreme Learning Machine (KELM) with a Mean-Variance Mapping Optimization (MVMO) algorithm was proposed. An MVMO was used to optimize the parameter settings of the KELM for the online estimation of the voltage stability. The model was trained considering several operating conditions including different generation-demand scenarios with three types of consumers (commercial, residential, and industrial) as well as N−1 contingencies. Figure 9 shows different operating points as a function of the real and reactive power demand, load increase directions, and contingencies. For each PQ bus of the IEEE 39 bus test network, active and reactive power demands were taken for a 24-h duration. Also, the uncertainty in the demand was considered using a probability density function (PDF) of a normal distribution. Then, an optimal power flow (OPF) was executed for each sample of the input variables to define a stable pre-contingency state scenario. Static N−1 contingency analysis and a continuation power flow (CPF) were executed to determine the VSM for both pre-and post-contingency conditions in the test system. The VSM corresponds to the maximum point of transfer in the P-V curve. The distance from the system operating point to the voltage instability frontier depends on the load increase trajectory and the initial operating point of the system and the occurrence of N−1 contingencies. Database training and model validation was performed through the Monte Carlo simulations.
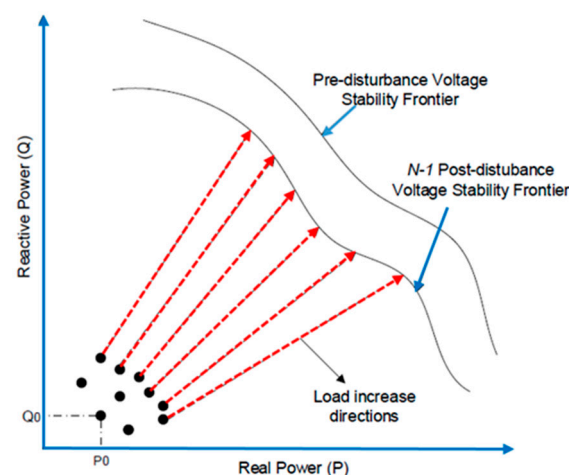

Figure 9. Voltage stability margin (VSM) variation [108].

3.1.4. Network-Load Admittance Ratio-Based VSI

Comparing to the traditional voltage stability index, which decreases sharply to zero just before the voltage stability limit, a linear voltage stability index was proposed in [109] for a generic distribution system utilizing the network-load admittance ratio that characterizes the system loading status. The network-load admittance ratio is in terms of the power network admittance matrix and the equivalent admittances of net loads, and the effects of constant-power and constant-current DGs are taken into consideration. Equation (24) gives a voltage stability index, $M_{n/d}$ under the condition that the power flow Jacobian is singular if, and only if, the network-load admittance ratio is unity, i.e., $R_{n/d} = 1$.

$$M_{n/d} = 1 - \frac{R_{n/d}|1 < \alpha_{loss} + 1 < \alpha_d|^2}{|1 < \alpha_{loss} + R_{n/d} < \alpha_d|^2} \tag{29}$$

where $R_{n/d}$ is network-load admittance ratio, α_{loss} is the power factor of the equivalent load impedance and α_d is the power factor of network loss. The values of α_{loss} and α_d are obtained from the following equations:

$$\alpha_{loss} = tan^{-1}\frac{Q_{loss}}{P_{loss}} \tag{30}$$

$$\alpha_d = tan^{-1}\frac{Q_d}{P_d} \tag{31}$$

Here, $R_{n/d}$ approaches to infinity at the zero load case and $R_{n/d} = 1$ at the voltage stability limit point, while the voltage stability index $M_{n/d}$ ranges from 0 (stability limit point) to 1 (zero load case).

4. Some Aspects of Voltage Stability of Power Systems with Embedded Microgrids

4.1. IBGs and System Strength

Concerning system strength, IBGs cannot support the grid as much as synchronous machines do. So, their connections to the grid negatively impact the system's strength. The North American Electric Reliability Corporation (NERC) has asserted in [110] that if IBGs are connected in weak regions, they will struggle to maintain tight control over real and reactive currents in periods immediately following fault clearing, resulting in the need to actively limit or even eliminate current injection until control can be restored. To accommodate the large amount of RESs, it is necessary to evaluate the system strength and prepare measures to cope with problems such as voltage instability. The concept of short-circuit ratio (SCR), which was first introduced by IEEE in 1997 [27], has conventionally been used to evaluate the system strength. This concept has also been used to evaluate system strength when an IBG is connected to the grid. However, the SCR does not reflect the interaction impact of IBGs. When several IBGs are concentrated in electrically connected areas, it becomes necessary to take into account the interaction of IBGs in the evaluation of system strength. Many studies were undertaken to tackle this issue. For example, references [111,112] have studied the case of voltage oscillations by renewable generators when connected to weak systems. In [113], the system strength was evaluated using the interaction factor for an integrated system based on inverters. Researchers in [114–116] proposed methods to overcome the disadvantage of the SCR approach. Other methods were developed, such as weighted short circuit ratio (WSCR) by the Electric Reliability Council of Texas (ERCOT), which takes into account the interaction between IBGs. The study in [117,118] contemplated the actual electrical interaction when IBGs are connected to nearby areas. For wind farms, extensive research was carried out on the voltage stability issues that occur when large wind farms are connected to weak grids, for example [119–122], which provide a measure of the system strength for renewable energy connections. However, most of the aforementioned methods for evaluating the system strength assumed that IBGs have a 100% interaction within a boundary. However, it is very difficult to calculate the boundary within the actual system. Therefore, to overcome these challenges, it is necessary to calculate the exact effect of nearby IBGs. In [123], a method is proposed to calculate the interaction level by tracking the output of IBGs by a power tracing method. It was asserted that the interaction level of the IBGs can more accurately estimate the system strength when the renewable generators are connected to adjacent points.

4.2. IBGs in Dual-Mode Operation

Another aspect of power systems with embedded microgrids is their voltage stability in dual-mode operation, i.e., MGs operating in grid-connected and islanded modes, and transition between these two modes. Voltage source inverters are generally used for transfer between these two modes. Commonly, dual-mode operated voltage source inverters use LC-type output filters for the islanded mode and use LCL-type output filters for grid-

connected mode. These filters may cause resonance in the inverters control systems and may result in instability issues. To mitigate the resonance of the filter, numerous control schemes were proposed in two categories, passive damping [124–126] and active damping [127]. The impact of different control schemes of an IBG on microgrid stability during and subsequent to fault-triggered islanding conditions is analyzed in [128], and the microgrid stability performance is examined with different load types. The main problem with the dual-mode voltage stability study is that the two operating modes cause different stability performances. The damping scheme designed for one mode may fail in another mode, thus causing system instability. To solve this problem, ref. [129] examined a voltage-controlled scheme for controlling the system at both operational modes. The stability performance of voltage source inverters under dual-mode operation was then investigated. The paper highlighted that for the traditional dual-loop control method, there exists a blind area of stability design, where the system cannot remain stable under the two modes simultaneously. Therefore, the article proposed a blind-area-free control design method and showed that the blind area of the traditional control method can be eliminated.

5. Example of Case Studies from the Literature

Many case studies were carried out to examine various proposed methods for voltage stability of power systems with microgrids. Here, only a few examples are presented.

In [130], a study was carried out on the static voltage stability impact of solar photovoltaic generation (SPVG) on power networks using P–V and V–Q curves to investigate the renewable energy generator model performance suitability. The analysis was done for the standard IEEE 14-Bus Benchmark Network, which is shown in Figure 10. The study evaluated the impact based on variable power factor control, variable static voltage droop control, increasing penetrations, and application of the concept of percentage change in voltage–power sensitivity to determine the best installation site for SPVG in the power system.
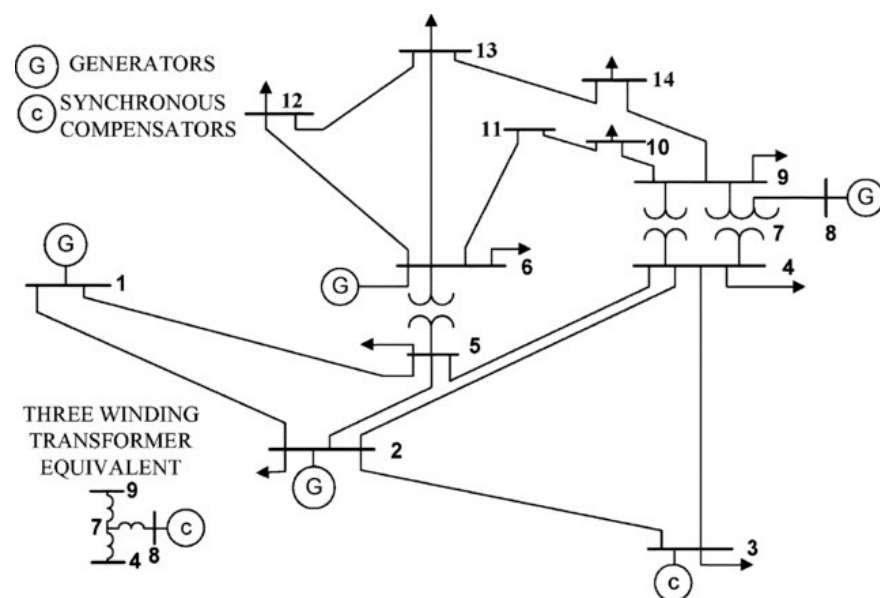

Figure 10. Single-line diagram of the IEEE 14-bus benchmark system [130].

In [131], the load-modified Nigerian power system model, shown in Figure 11, was used as a case study for determining optimal penetration of utility-scale PV solar power into the power system considering voltage stability.
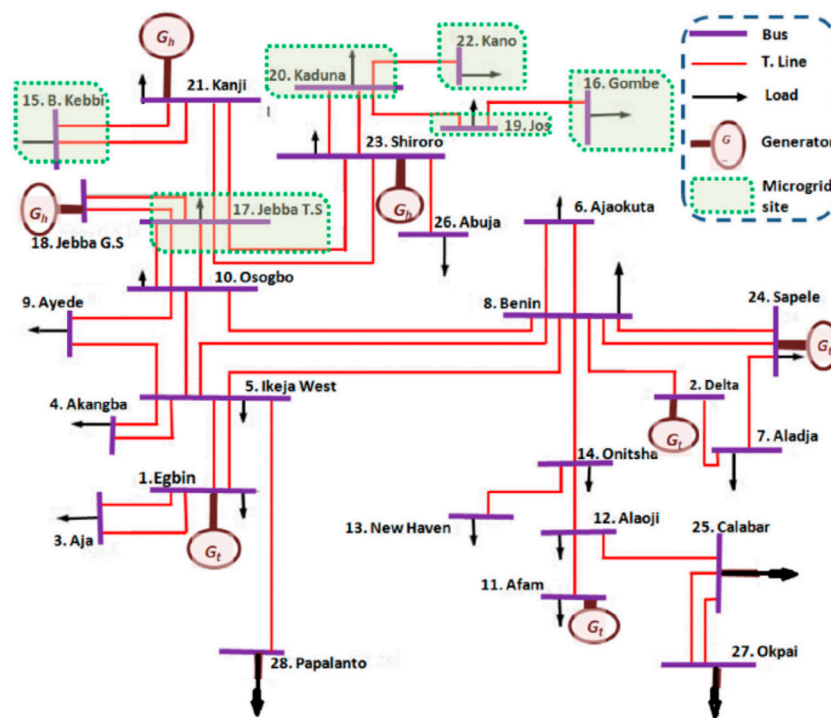
Figure 11. Nigerian power system with highlighted microgrid site and other PV solar farm sites [131].

The performance of two cases with different objective functions was compared to establish the best practice for achieving voltage stability at a reasonable cost and without compromising system reliability. In case 1, only the line loss minimization approach was used in the optimization objective function. In case 2, an additional constraint based on voltage stability margin was included to keep the system within the stability margin. Overall, the results showed that incorporating voltage stability conditions into the objective functions could achieve a better system performance in terms of reliability, cost-saving, and power system security.

In [25], a voltage support strategy was presented for grid-feeding PV inverter to improve the dynamic voltage stability of islanded MG. Two islanded MGs were used as case studies to investigate the effectiveness of the proposed strategy. The second case was more complete compared to the first one and was made by modifying the IEEE 15-bus test system by adding DGs and induction motor loads. Figure 12 shows this case study, which was used to demonstrate the effectiveness of a coordinated and optimized active and reactive power control for stabilizing the DVS of an islanded MG.

A CIGRE benchmark test system was used in [132] as a case study to demonstrate the performance of a multi-objective voltage stability-constrained microgrid energy management system. This case study is shown in Figure 13.

One important observation that this paper has made is about the customers' influence on voltage stability through demand response programs. When the participation of customers increases, the system voltage stability improves.
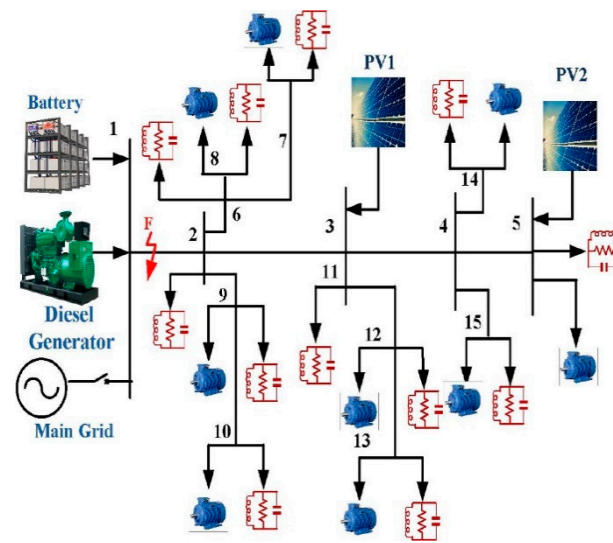
Figure 12. Case study as a microgrid system for investigating dynamic voltage stability [25].
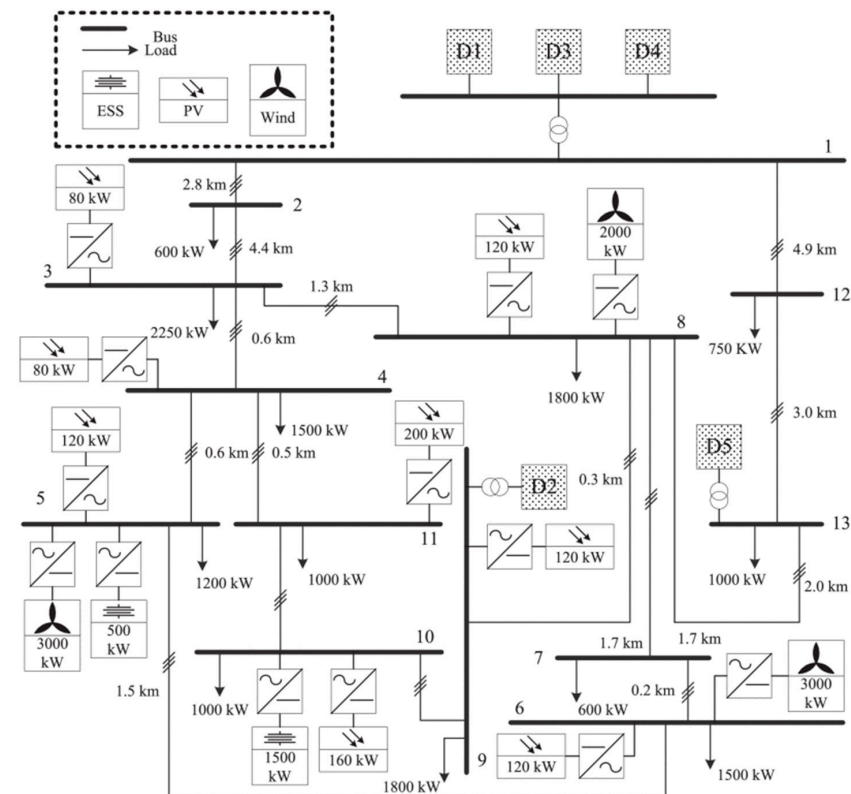

Figure 13. A CIGRE microgrid benchmark test system [132].

6. Conclusions

This article has presented a comprehensive review on voltage stability of microgrids (MGs) as integral components of a modern power grid. It reviewed the literature on the impact of microgrid topologies on the voltage stability of microgrids and of the power system to which the MGs are connected. The review includes voltage stability of autonomous AC and DC MGs, and grid-connected AC and DC MGs. Other subjects reviewed in this article are the impact of interlinking converters, DC-link voltage, islanded microgrids, size and duration of disturbances, coordination of voltage control loops, and load dynamics on voltage stability. Methods of static and dynamic analysis for determining voltage stability of microgrids are presented. Voltage stability indices for microgrids are reviewed.

Some aspects of voltage stability of power systems with embedded microgrids are studied including the effect of system strength on the stability of IBGs, and stability of IBGs in dual-mode operation. Finally, a review of some case studies that have been carried out in the literature to examine various proposed methods for voltage stability of power systems integrated with microgrids is presented.

References

1. CIGRE. Microgrids 1 Engineering, Economics, & Experience. In *Conseil International des Grands Réseaux Electriques*; CIGRÉ: Paris, France, 2015.
2. IEEE PES Task Force on Microgrid Stability Analysis and Modeling. *Microgrid Stability, Definitions, Analysis, and Modeling*; IEEE PES: Piscataway, NJ, USA, 2008.
3. Beheshtaein, S.; Savaghebi, M.; Vasquez, J.C.; Guerrero, J.M. Protection of AC and DC microgrids: Challenges, solutions and future trends. In Proceedings of the IECON 2015–41st Annual Conference of the IEEE Industrial Electronics Society, Yokohama, JP, USA, 9–12 November 2015; pp. 5253–5260. [CrossRef]
4. Basak, P.; Chowdhury, S.; Halder Nee Dey, S.; Chowdhury, S.P. A literature review on integration of distributed energy resources in the perspective of control, protection and stability of microgrid. *Renew. Sustain. Energy Rev.* **2012**, *16*, 5545–5556. [CrossRef]
5. Bhaskara, S.N.; Chowdhury, B.H. Microgrids—A review of modeling, control, protection, simulation and future potential. *IEEE Power Energy Soc. Gen. Meet.* **2012**. [CrossRef]
6. Hossain, M.A.; Pota, H.R.; Hossain, M.J.; Blaabjerg, F. Evolution of microgrids with converter-interfaced generations: Challenges and opportunities. *Int. J. Electr. Power Energy Syst.* **2019**, *109*, 160–186. [CrossRef]
7. Schiffer, J.; Ortega, R.; Astolfi, A.; Raisch, J.; Sezi, T. Conditions for stability of droop-controlled inverter-based microgrids. *Automatica* **2014**, *50*, 2457–2469. [CrossRef]
8. Leitner, S.; Yazdanian, M.; Mehrizi-Sani, A.; Muetze, A. Small-signal stability analysis of an inverter-based microgrid with internal model-based controllers. *IEEE Trans. Smart Grid* **2017**, *9*, 5393–5402. [CrossRef]
9. Bottrell, N.; Prodanovic, M.; Green, T.C. Dynamic stability of a microgrid with an active load. *IEEE Trans. Power Electron.* **2013**, *28*, 5107–5119. [CrossRef]
10. Kroposki, B.; Lasseter, R.; Ise, T.; Morozumi, S.; Papathanassiou, S.; Hatziargyriou, N. Making microgrids work. *IEEE Power Energy Mag.* **2008**, *6*, 40–53. [CrossRef]
11. Diaz, N.L.; Dragicevic, T.; Vasquez, J.C.; Guerrero, J.M. Intelligent distributed generation and storage units for DC microgrids—A new concept on cooperative control without communications beyond droop control. *IEEE Trans. Smart Grid* **2014**, *5*, 2476–2485. [CrossRef]
12. Guerrero, J.M.; Vasquez, J.C.; Matas, J.; de Vicuña, L.G.; Castilla, M. Hierarchical control of droop-controlled AC and DC microgrids—A general approach toward standardization. *IEEE Trans. Ind. Electron.* **2010**, *58*, 158–172. [CrossRef]
13. Sanduleac, M.; Toma, L.; Eremia, M.; Ciorner, I.; Bulac, C.; Tristiu, I.; Lantoc, A.; Martins, J.F. On the electrostatic inertia in microgrids with inverter-based generation only—An analysis on dynamic stability. *Energies* **2019**, *12*, 3274. [CrossRef]
14. Bullich-Massagué, E.; Díaz-González, F.; Aragüés-Peñalba, M.; Girbau-Llistuella, F.; Olivella-Rosell, P.; Sumper, A. Microgrid clustering architectures. *Appl. Energy* **2018**, *212*, 340–361. [CrossRef]
15. Hatziargyriou, N.; Dimeas, A.; Tsikalakis, A. Centralized and decentralized control of microgrids. *Int. J. Distrib. Energy Resour.* **2005**, *1*, 197–212.
16. Katiraei, F.; Iravani, M.R.; Lehn, P. Microgrid autonomous operation during and subsequent to islanding process. *IEEE Power Eng. Soc. Gen. Meet.* **2004**, *2*, 2175.
17. Mahmoud, M.S. Microgrid Control Problems and Related Issues. In *Microgrid: Advanced Control Methods and Renewable Energy System Integration*; Elsevier: Amsterdam, The Netherlands, 2017; Chapter 1; pp. 1–42.
18. Islam, M.; Mithulananthan, N.; Hossain, M.J. Dynamic voltage support by TL-PV systems to mitigate short-term voltage instability in residential DN. *IEEE Trans. Power Syst.* **2017**, *33*, 4360–4370. [CrossRef]
19. Varma, R.K.; Siavashi, E.M. PV-STATCOM: A new smart inverter for voltage control in distribution systems. *IEEE Trans. Sustain. Energy* **2018**, *9*, 1681–1691. [CrossRef]
20. Kawabe, K.; Ota, Y.; Yokoyama, A.; Tanaka, K. Novel dynamic voltage support capability of photovoltaic systems for improvement of short-term voltage stability in power systems. *IEEE Trans. Power Syst.* **2016**, *32*, 1796–1804. [CrossRef]
21. Islam, M.; Nadarajah, M.; Hossain, M.J. Short-term voltage stability enhancement in residential grid with high penetration of rooftop PV units. *IEEE Trans. Sustain. Energy* **2018**, *10*, 2211–2222. [CrossRef]

22. Alaboudy, A.H.K.; Zeineldin, H.H.; Kirtley, J. Simple control strategy for inverter-based distributed generator to enhance microgrid stability in the presence of induction motor loads. *IET Gener. Transm. Distrib.* **2013**, *7*, 1155–1162. [CrossRef]

23. Farrokhabadi, M.; Cañizares, C.A.; Simpson-Porco, J.W.; Nasr, E.; Fan, L.; Mendoza-Araya, P.A.; Tonkoski, R.; Tamrakar, U.; Hatziargyriou, N.; Lagosal, D.; et al. Microgrid stability definitions, analysis, and examples. *IEEE Trans. Power Syst.* **2020**, *35*, 13–29. [CrossRef]

24. Afrin, N.; Yang, F.; Lu, J. Optimized reactive power support strategy for photovoltaic inverter to intensify the dynamic voltage stability of islanded microgrid. *Int. Trans. Electr. Energy Syst.* **2020**, *30*, e12356. [CrossRef]

25. Ayaz, M.S.; Azizipanah-Abarghooee, R.; Terzija, V. European LV microgrid benchmark network: Development and frequency response analysis. In Proceedings of the 2018 IEEE International Energy Conference, Limassol, Cyprus, 3–7 June 2018; pp. 1–6.

26. Afrin, N.; Yang, F.; Lu, J. Voltage support strategy for PV inverter to enhance dynamic voltage stability of islanded microgrid. *Int. J. Electr. Power Energy Syst.* **2020**, *121*, 106059. [CrossRef]

27. IEEE Standards. IEEE Guide for Planning DC Links Terminating at AC Locations Having Low Short-Circuit Capacities. In *IEEE Std 1204-1997*; IEEE: Piscataway, NJ, USA, 1997; pp. 1–216. [CrossRef]

28. Golieva, A. Low Short-Circuit Ratio Connection of Wind Power Plants. Mater's Thesis, Norwegian University of Science and Technology (NTNU), Trondheim, Norway, 2015.

29. ANSI. *Electric Power Systems and Equipment Voltage Ratings (60 Hertz)*; The American National Standard Institute (ANSI): Piscataway, NJ, USA, 2011.

30. Weaver, W.W.; Krein, P.T. Mitigation of power system collapse through active dynamic buffers. In Proceedings of the 2004 IEEE 35th Annual Power Electronics Specialists Conference (IEEE Cat. No. 04CH37551), Aachen, Germany, 20–25 June 2004; IEEE: Aachen, Germany, 2004; Volume 2, pp. 1080–1084.

31. Sanduleac, M.; Martins, J.F.; Ciornei, I.; Albu, M.; Toma, L.; Pires, V.F.; Hadjidemetriou, L.; Sauba, R. Resilient and immune by design microgrids using solid state transformers. *Energies* **2018**, *11*, 3377. [CrossRef]

32. Anand, S.; Fernandes, B.G.; Guerrero, J. Distributed Control to Ensure Proportional Load Sharing and Improve Voltage Regulation in Low-Voltage DC Microgrids. *IEEE Trans. Power Electron.* **2013**, *28*, 1900–1913. [CrossRef]

33. Papadimitriou, C.N.; Zountouridou, E.I.; Hatziargyriou, N.D. Review of hierarchical control in DC microgrids. *Electr. Power Syst. Res.* **2015**, *122*, 159–167. [CrossRef]

34. Neto, P.J.d.S.; Barros, T.A.S.; Silveira, J.P.C.; Filho, E.R.; Vasquez, J.C.; Guerrero, J.M. Power management techniques for grid-connected DC microgrids: A comparative evaluation. *Appl. Energy* **2020**, *269*. [CrossRef]

35. Kleftakis, V.; Lagos, D.; Papadimitriou, C.; Hatziargyriou, N.D. Seamless Transition between Interconnected and Islanded Operation of DC Microgrids. *IEEE Trans. Smart Grid* **2019**, *10*, 248–256. [CrossRef]

36. Liu, Z.; Liu, R.; Zhang, X.; Su, M.; Sun, Y.; Han, H.; Wang, P. Feasible power-flow solution analysis of DC microgrids under droop control. *IEEE Trans. Smart Grid* **2020**, *11*, 2771. [CrossRef]

37. Xie, W.; Han, M.; Cao, W.; Guerrero, J.M.; Vasquez, J.C. System-Level Large-Signal Stability Analysis of Droop-Controlled DC Microgrids. *IEEE Trans. Power Electron.* **2021**, *36*, 4224. [CrossRef]

38. Liu, G.; Caldognetto, T.; Mattavelli, P.; Magnone, P. Power-Based Droop Control in DC Microgrids Enabling Seamless Disconnection From Upstream Grids. *IEEE Trans. Power Electron.* **2019**, *34*, 2039. [CrossRef]

39. Chen, D.; Xu, Y.; Huang, A.Q. Integration of DC Microgrids as Virtual Synchronous Machines Into the AC Grid. *IEEE Trans. Ind. Electron.* **2017**, *64*, 7455. [CrossRef]

40. Zhang, L.; Tai, N.; Huang, W.; Liu, J.; Wang, Y. A review on protection of DC microgrids. *J. Mod. Power Syst. Clean Energy* **2018**, *6*, 1113. [CrossRef]

41. Tah, A.; Das, D. An Enhanced Droop Control Method for Accurate Load Sharing and Voltage Improvement of Isolated and Interconnected DC Microgrids. *IEEE Trans. Sustain. Energy* **2016**, *7*, 1194–1204. [CrossRef]

42. Nasirian, V.; Moayedi, S.; Davoudi, A.; Lewis, F.L. Distributed Cooperative Control of DC Microgrids. *IEEE Trans. Power Electron.* **2015**, *30*, 2288–2303. [CrossRef]

43. Dragičević, T.; Lu, J.C.V.X.; Guerrero, J.M. DC Microgrids—Part I: A Review of Control Strategies and Stabilization Techniques. *IEEE Trans. Power Electron.* **2016**, *31*, 4876–4891.

44. Shuai, Z.; Fang, J.; Ning, F.; Shen, Z.J. Hierarchical structure and bus voltage control of DC microgrid. *Renew. Sustain. Energy Rev.* **2018**, *82*, 3670–3682. [CrossRef]

45. Meng, L.; Shafiee, Q.; Ferrari Trecate, G.; Karimi, H.; Fulwani, D.; Lu, X.; Guerrero, J.M. Review on Control of DC Microgrids and Multiple Microgrid Clusters. *IEEE J. Emerg. Sel. Top. Power Electron.* **2017**, *5*, 928–948.

46. Meng, L.; Dragicevic, T.; Vasquez, J.C.; Guerrero, J.M. Tertiary and Secondary Control Levels for Efficiency Optimization and System Damping in Droop Controlled DC–DC Converters. *IEEE Trans. Smart Grid* **2015**, *6*, 2615–2626. [CrossRef]

47. Chen, F.; Burgos, R.; Boroyevich, D.; Vasquez, J.C.; Guerrero, J.M. Investigation of Nonlinear Droop Control in DC Power Distribution Systems. *IEEE Trans. Power Electron.* **2019**, *34*, 9404–9421. [CrossRef]

48. Farasat, M.; Mehraeen, S.; Arabali, A.; Trzynadlowski, A. GA-based optimal power flow for microgrids with DC distribution network. In Proceedings of the IEEE Energy Conversion Congress and Exposition (ECCE), Montreal, QC, Canada, 20–24 September 2015; pp. 3372–3379.

49. Peyghami, S.; Mokhtari, H.; Blaabjerg, F. Hierarchical power sharing control in DC microgrids. In *Microgrid*; Elsevier: Amsterdam, The Netherlands, 2017; pp. 63–100.

50. Issa, W.; Al-naemi, F.; Konstantopoulos, G.; Sharkh, S.; Abusara, M. Stability Analysis and Control of a Microgrid against Circulating Power between Parallel Inverters. *Energy Procedia* **2019**, *157*, 1061–1070. [CrossRef]
51. Loh, P.C.; Li, Y.K.C.D.; Blaabjerg, F. Autonomous operation of hybrid microgrid with ac and dc subgrids. *IEEE Trans. Power Electron.* **2013**, *28*, 2214–2223. [CrossRef]
52. Kundur, P.; Balu, N.J.; Lauby, M.G. *Power System Stability and Control*; McGraw-Hill: New York, NY, USA, 1994.
53. Emadi, A.; Khaligh, A.; Rivetta, C.H.; Williamson, G.A. Constant power loads and negative impedance instability in automotive systems: Definition, modeling, stability, and control of power electronic converters and motor drives. *IEEE Trans. Veh. Technol.* **2006**, *55*, 1112–1125. [CrossRef]
54. Al-Nussairi, M.K.; Bayindir, R.; Padmanaban, S.; Mihet-Popa, L.; Siano, P. Constant power loads (CPL) with Microgrids: Problem definition, stability analysis and compensation techniques. *Energies* **2017**, *10*, 1656. [CrossRef]
55. Lin, L.; Zhao, X.; Zhu, J.; Zhang, X.; Yang, R. Simulation Analysis of Microgrid Voltage Stability with Multi-induction Motor Loads. *Electr. Power Compon. Syst.* **2018**, *46*, 560–569. [CrossRef]
56. Eremia, M.; Shahidehpour, M. *Handbook of Electrical Power System Dynamics: Modeling, Stability, and Control*; Wiely: Hoboken, NJ, USA, 2013.
57. Solanki, B.V.; Canizares, C.A.; Bhattacharya, K. Practical Energy Management Systems for Isolated Microgrids. *IEEE Trans. Smart Grid* **2018**. [CrossRef]
58. Eajal, A.A.; Yazdavar, A.H.; El-Saadany, E.F.; Ponnambalam, K. On the Loadability and Voltage Stability of Islanded AC–DC Hybrid Microgrids during Contingencies. *IEEE Syst. J.* **2019**, *13*, 4248–4259. [CrossRef]
59. Sao, C.K.; Lehn, P.W. Autonomous load sharing of voltage source converters. *IEEE Trans. Power Deliv.* **2005**, *20*, 1009–1016. [CrossRef]
60. Guerrero, J.M.; Chandorkar, M.; Lee, T.-L.; Loh, P.C. Advanced control architectures for intelligent microgrids—Part I: Decentralized and hierarchical control. *IEEE Trans. Ind. Electron.* **2012**, *60*, 1254–1262. [CrossRef]
61. Ghalebani, P.; Niasati, M. A distributed control strategy based on droop control and low-bandwidth communication in DC microgrids with increased accuracy of load sharing. *Sustain. Cities Soc.* **2018**, *40*, 155–164. [CrossRef]
62. Nasirian, V.; Davoudi, A.; Lewis, F.L. Distributed adaptive droop control for DC microgrids. In Proceedings of the IEEE Applied Power Electronics Conference and Exposition–APEC, Fort Worth, TX, USA, 16–20 March 2014; pp. 1147–1152. [CrossRef]
63. Chiang, H.D.; Jean-Jumeau, R. Toward a Practical Performance Index for Predicting Voltage Collapse in Electric Power Systems. *IEEE Trans. Power Syst.* **1995**, *10*, 584–592. [CrossRef]
64. Machowski, J.; Lubosny, Z.; Bialek, J.W.; Bumby, J.R. *Power System Dynamics: Stability and Control*; John Wiley & Sons: Hoboken, NJ, USA, 2020.
65. Togiti, V. *Pattern Recognition of Power System Voltage Stability Using Statistical and Algorithmic Methods*; LAP LAMBERT Academic Publishing: Saarbrücken, Germany, 2012.
66. Rashid, A. Voltage Stability Analysis with High Distributed Generation (DG) Penetration. Ph.D. Thesis, University of Waterloo, Waterloo, ON, Canada, 2012.
67. Ren, L.; Zhang, P. Generalized microgrid power flow. *IEEE Trans. Smart Grid* **2018**, *9*, 3911–3913. [CrossRef]
68. Nocedal, J.; Wright, S. *Numerical Optimization*; Springer Science & Business Media: Berlin/Heidelberg, Germany, 2006.
69. Beerten, J.; Cole, S.; Belmans, R. Generalized steady-state VSC MTDC model for sequential AC/DC power flow algorithms. *IEEE Trans. Power Syst.* **2012**, *27*, 821–829. [CrossRef]
70. Baradar, M.; Ghandhari, M. A multi-option unified power flow approach for hybrid AC/DC grids incorporating multi-terminal VSC-HVDC. *IEEE Trans. Power Syst.* **2013**, *28*, 2376–2383. [CrossRef]
71. Eajal, A.A. The New AC/DC Hybrid Microgrid Paradigm: Analysis and Operational Control. Ph.D. Thesis, University of Waterloo, Waterloo, ON, Canada, 2018.
72. Wang, L.Y.; Polis, M.; Wang, C.; Lin, F. Voltage stability and robustness for microgrid systems. In Proceedings of the 2013 European Control Conference, Zurich, Switzerland, 17–19 July 2013; pp. 2038–2043. [CrossRef]
73. Kordkheili, H.H.; Banejad, M.; Kalat, A.A.; Pouresmaeil, E.; Catalão, J.P.S. Direct-lyapunov-based control scheme for voltage regulation in a three-phase islanded microgrid with renewable energy sources. *Energies* **2018**, *11*, 1161. [CrossRef]
74. Shuai, Z.; Peng, Y.; Liu, X.; Li, Z.; Guerrero, J.M.; Shen, Z.J. Parameter stability region analysis of islanded microgrid based on bifurcation theory. *IEEE Trans. Smart Grid* **2019**, *10*, 6580–6591. [CrossRef]
75. Majumder, R. Some aspects of stability in microgrids. *IEEE Trans. Power Syst.* **2013**, *28*, 3243–3252. [CrossRef]
76. Modarresi, J.; Gholipour, E.; Khodabakhshian, A. A comprehensive review of the voltage stability indices. *Renew. Sustain. Energy Rev.* **2016**, *63*, 1–12. [CrossRef]
77. Ettehadi, M.; Ghasemi, H.; Vaez-Zadeh, S. Voltage stability-based DG placement in distribution networks. *IEEE Trans. Power Deliv.* **2013**, *28*, 171–178. [CrossRef]
78. Rao, A.R.N.; Vijaya, P.; Kowsalya, M. Voltage stability indices for stability assessment: A Review. *Int. J. Ambient. Energy* **2018**, 1–17. [CrossRef]
79. Mahmud, M.A.; Hossain, J.; Pota, H.R. Voltage variation on distribution networks with distributed generation: Worst case scenario. *IEEE Syst. J.* **2013**, *8*, 1096–1103. [CrossRef]
80. Musirin, I.; Rahman, T.K.A. Novel fast voltage stability index (FVSI) for voltage stability analysis in power transmission system. In Proceedings of the Student Conference on Research and Development, Shah Alam, Malaysia, 16–17 July 2002; pp. 265–268.

81. Subramani, C.; Dash, S.; Bhaskar, M.A.; Jagadeeshkumar, M.; Sureshkumar, K.; Parthipan, R. Line outage contingency screening and ranking for voltage stability assessment. In Proceedings of the 2009 International Conference on Power Systems, Kharagpur, India, 27–29 December 2009; pp. 1–5.

82. Moghavvemi, M.; Omar, F.M. Technique for contingency monitoring and voltage collapse prediction. *IEEE Proc. Gener. Transm. Distrib.* **1998**, *145*, 634–640. [CrossRef]

83. Moghavvemi, M.; Faruque, M.O. Technique for assessment of voltage stability in ill-conditioned radial distribution network. *IEEE Power Eng. Rev.* **2001**, *21*, 58–60. [CrossRef]

84. Aman, M.M.; Jasmon, G.B.; Mokhlis, H.; Bakar, A.H.A. Optimal placement and sizing of a DG based on a new power stability index and line losses. *Int. J. Electr. Power Energy Syst.* **2012**, *43*, 1296–1304. [CrossRef]

85. Moghavvemi, M.; Faruque, O. Real-time contingency evaluation and ranking technique. *IEEE Proc. Gener. Transm. Distrib.* **1998**, *145*, 517–524. [CrossRef]

86. Wang, L.; Liu, Y.; Luan, Z. Power transmission paths based voltage stability assessment. In Proceedings of the 2005 IEEE/PES Transmission & Distribution Conference & Exposition: Asia and Pacific, New Orleans, LA, USA, 9–14 October 2005; pp. 1–5.

87. Yazdanpanah-Goharrizi, A.; Asghari, R. A novel line stability index (NLSI) for voltage stability assessment of power systems. In Proceedings of the 7th WSEAS International Conference on Power Systems, Stevens, WI, USA, 21–23 November 2007; pp. 164–167.

88. Kanimozhi, R.; Selvi, K. A novel line stability index for voltage stability analysis and contingency ranking in power system using fuzzy based load flow. *J. Electr. Eng. Technol.* **2013**, *8*, 694–703. [CrossRef]

89. Althowibi, F.A.; Mustafa, M.W. Ine voltage stability calculations in power systems. In Proceedings of the 2010 IEEE International Conference on Power and Energy, Kuala Lumpur, Malaysia, 29 Novenber–1 December 2010; pp. 396–401.

90. Makasa, K.J.; Venayagamoorthy, G.K. On-line voltage stability load index estimation based on PMU measurements. In Proceedings of the 2011 IEEE Power and Energy Society General Meeting, Detroit, MI, USA, 24–29 July 2011; pp. 1–6.

91. Gong, Y.; Schulz, N.; Guzman, A. Synchrophasor-based real-time voltage stability index. In Proceedings of the 2006 IEEE PES Power Systems Conference and Exposition, Atlanta, GA, USA, 29 October–1 November 2006; IEEE: Atlanta, GA, USA, 2006; pp. 1029–1036.

92. Chattopadhyay, T.K.; Banerjee, S.; Chanda, C.K. Impact of distributed generator on voltage stability analysis of distribution networks under critical loading conditions. In Proceedings of the 2014 1st International Conference on Non Conventional Energy (ICONCE 2014), Kalyani, India, 16–17 January 2014; pp. 288–291.

93. Deng, P.; Sun, Y.; Xu, J. A new index of voltage stability considering distribution network. In Proceedings of the 2009 Asia-Pacific Power and Energy Engineering Conference, Wuhan, China, 28–31 March 2009; pp. 1–4.

94. He, T.; Kolluri, S.; Mandal, S.; Galvan, F.; Rasigoufard, P. Identification of weak locations in bulk transmission systems using voltage stability margin index. In Proceedings of the IEEE Power Engineering Society General Meeting, Denver, CO, USA, 6–10 June 2004; pp. 1814–1819.

95. Tiwari, R.; Niazi, K.; Gupta, V. Line collapse proximity index for prediction of voltage collapse in power systems. *Int. J. Electr. Power Energy Syst.* **2012**, *41*, 105–111. [CrossRef]

96. Nizam, M.; Mohamed, A.; Hussain, A. Dynamic voltage collapse prediction in power systems using power transfer stability index. In Proceedings of the 2006 IEEE International Power and Energy Conference, Putrajaya, Malaysia, 28–29 November 2006; pp. 246–250.

97. Balamourougan, V.; Sidhu, T.S.; Sachdev, M.S. Technique for online prediction of voltage collapse. *IEE Proc. Gener. Transm. Distrib.* **2004**, *151*, 453–460. [CrossRef]

98. Micky, R.R.; Lakshmi, R.; Sunitha, R.; Ashok, S. Assessment of voltage stability in microgrid. In Proceedings of the 2016 International Conference on Electrical, Electronics, and Optimization Techniques (ICEEOT), Chennai, India, 3–5 March 2016; pp. 1268–1273.

99. Kessel, P.; Glavitsch, H. Estimating the voltage stability of a power system. *IEEE Trans. Power Deliv.* **1986**, *1*, 346–354. [CrossRef]

100. Haque, M.H. Use of local information to determine the distance to voltage collapse. *Int. J. Emerg. Electr. Power Syst.* **2008**, *9*, 2. [CrossRef]

101. Pérez-Londoño, S.; Rodríguez, L.; Olivar, G. A simplified voltage stability index (SVSI). *Int. J. Electr. Power Energy Syst.* **2014**, *63*, 806–813. [CrossRef]

102. Verbic, G.; Gubina, F. A new concept of voltage-collapse protection based on local phasors. *IEEE Trans. Power Deliv.* **2004**, *19*, 576–581. [CrossRef]

103. Smon, I.; Verbic, G.; Gubina, F. Local voltage-stability index using Tellegen's theorem. *IEEE Trans. Power Syst.* **2006**, *21*, 1267–1275. [CrossRef]

104. Wiszniewski, A. New criteria of voltage stability margin for the purpose of load shedding. *IEEE Trans. Power Deliv.* **2007**, *22*, 1367–1371. [CrossRef]

105. Matavalam, A.R.R.; Singhal, A.; Ajjarapu, V. Monitoring Long Term Voltage Instability Due to Distribution and Transmission Interaction Using Unbalanced μ PMU and PMU Measurements. *IEEE Trans. Smart Grid* **2019**, *11*, 873–883. [CrossRef]

106. England, B.S.; Alouani, A.T. Real time voltage stability prediction of smart grid areas using smart meters data and improved Thevenin estimates. *Int. J. Electr. Power Energy Syst.* **2020**, *122*, 106189. [CrossRef]

107. Katsanevakis, M.; Stewart, R.A.; Junwei, L. A novel voltage stability and quality index demonstrated on a low voltage distribution network with multifunctional energy storage systems. *Electr. Power Syst. Res.* **2019**, *171*, 264–282. [CrossRef]

108. Villa-Acevedo, W.M.; López-Lezama, J.M.; Colomé, D.G. Voltage Stability Margin Index Estimation Using a Hybrid Kernel Extreme Learning Machine Approach. *Energies* **2020**, *13*, 857. [CrossRef]

109. Song, Y.; Hill, D.J.; Liu, T. Static voltage stability analysis of distribution systems based on network-load admittance ratio. *IEEE Trans. Power Syst.* **2018**, *34*, 2270–2280. [CrossRef]

110. NERC. *Reliability Guideline: BPS-Connected Inverter-Based Resource Performance*; North American Electric Reliability Corporation (NERC): Atlanta, GA, USA, 2018.

111. NERC. *Integrating Inverter-Based Resources into Low Short Circuit Strength Systems*; North American Electric Reliability Corporation (NERC): Atlanta, GA, USA, 2017.

112. CIGRÉ. *Connection of Wind Farms to Weak AC Networks*; Conseil International des Grands Réseaux Electriques (CIGRÉ): Paris, France, 2016.

113. Saad, H.; Dennetière, S.; Clerc, B. *Interactions Investigations between Power Electronics Devices Embedded in HVAC Network*; IET: Manchester, UK, 2017.

114. Huang, S.-H.; Schmall, J.; Conto, J.; Adams, J.; Zhang, Y.; Carter, C. Voltage control challenges on weak grids with high penetration of wind generation: ERCOT experience. In Proceedings of the 2012 IEEE Power and Energy Society General Meeting, San Diego, CA, USA, 22–26 July 2012; pp. 1–7.

115. Zhang, Y.; Huang, S.-H.F.; Schmall, J.; Conto, J.; Billo, J.; Rehman, E. Evaluating system strength for large-scale wind plant integration. In Proceedings of the 2014 IEEE PES General Meeting\Conference & Exposition, National Harbor, MD, USA, 27–31 July 2014; pp. 1–5.

116. Huang, F. Experience with WTG weak system interactions on the ERCOT system. In Proceedings of the 2015 IEEE Power & Energy Society General Meeting, Denver, CO, USA, 26–30 July 2015; pp. 16–30.

117. Wu, D.; Li, G.; Javadi, M.; Malyscheff, A.M.; Hong, M.; Jiang, J.N. Assessing impact of renewable energy integration on system strength using site-dependent short circuit ratio. *IEEE Trans. Sustain. Energy* **2017**, *9*, 1072–1080. [CrossRef]

118. Wu, D.; Javadi, M.; Ma, F.; Tan, J.; Jiang, J.N. A method to identify weak points of interconnection of renewable energy resources. *Int. J. Electr. Power Energy Syst.* **2019**, *110*, 72–82. [CrossRef]

119. Zhou, F.; Joos, G.; Abbey, C. Voltage stability in weak connection wind farms. In Proceedings of the IEEE Power Engineering Society General Meeting 2005, San Francisco, CA, USA, 12–16 June 2005; pp. 1483–1488.

120. Fischer, M.; Schellschmidt, M. Fault ride through performance of wind energy converters with FACTS capabilities in response to up-to-date German grid connection requirements. In Proceedings of the 2011 IEEE/PES Power Systems Conference and Exposition, Phoenix, AZ, USA, 20–23 March 2011; pp. 1–6.

121. Piwko, R.; Miller, N.; Sanchez-Gasca, J.; Yuan, X.; Dai, R.; Lyons, J. Integrating large wind farms into weak power grids with long transmission lines. In Proceedings of the 2006 CES/IEEE 5th International Power Electronics and Motion Control Conference, Shanghai, China, 14–16 August 2006; Volume 2, pp. 1–7.

122. Diedrichs, V.; Beekmann, A.; Adloff, S. Loss of (angle) stability of wind power plants—The underestimated phenomenon in case of very low short circuit ratio. In Proceedings of the 10th International Workshop Large-Scale Integration Wind Power Power System Transmission Networks Offshore Wind Power Plants, Aarhus, Denmark, 25–26 October 2011; pp. 340–393.

123. Kim, D.; Cho, H.; Park, B.; Lee, B. Evaluating Influence of Inverter-based Resources on System Strength Considering Inverter Interaction Level. *Sustainability* **2020**, *12*, 3469. [CrossRef]

124. Wu, W.; He, Y.; Tang, T.; Blaabjerg, F. A new design method for the passive damped LCL and LLCL filter-based single-phase grid-tied inverter. *IEEE Trans. Ind. Electron.* **2012**, *60*, 4339–4350. [CrossRef]

125. Pena-Alzola, R.; Liserre, M.; Blaabjerg, F.; Sebastián, R.; Dannehl, J.; Fuchs, F.W. Analysis of the passive damping losses in LCL-filter-based grid converters. *IEEE Trans. Power Electron.* **2012**, *28*, 2642–2646. [CrossRef]

126. Cespedes, M.; Xing, L.; Sun, J. Constant-power load system stabilization by passive damping. *IEEE Trans. Power Electron.* **2011**, *26*, 1832–1836. [CrossRef]

127. Parker, S.G.; McGrath, B.P.; Holmes, D.G. Regions of active damping control for LCL filters. *IEEE Trans. Ind. Appl.* **2013**, *50*, 424–432. [CrossRef]

128. Alaboudy, A.H.K.; Zeineldin, H.H.; Kirtley, J. Microgrid stability characterization subsequent to fault-triggered islanding incidents. *IEEE Trans. Power Deliv.* **2012**, *27*, 658–669. [CrossRef]

129. Zhou, Z.; Li, X.; Lu, Y.; Liu, Y.; Shen, G.; Wu, X. Stability Blind-Area-Free Control Design for Microgrid-Interfaced Voltage Source Inverters under Dual-Mode Operation. *IEEE Trans. Power Electron.* **2020**, *35*, 12555–12569. [CrossRef]

130. Muhammed, A.O.; Rawa, M. A Systematic PVQV-Curves approach for investigating the impact of solar photovoltaic-generator in power system using powerworld simulator. *Energies* **2020**, *13*, 2662. [CrossRef]

131. Adewuyi, O.B.; Shigenobu, R.; Senjyu, T.; Lotfy, M.E.; Howlader, A. Multiobjective mix generation planning considering utility-scale solar PV system and voltage stability: Nigerian case study. *Electr. Power Syst. Res.* **2019**, *168*, 269–282. [CrossRef]

132. Nasr, M.-A.; Nikkhah, S.; Gharehpetian, G.B.; Nasr-Azadani, E.; Hosseinian, S.H. A multi-objective voltage stability constrained energy management system for isolated microgrids. *Int. J. Electr. Power Energy Syst.* **2020**, *117*, 105646. [CrossRef]